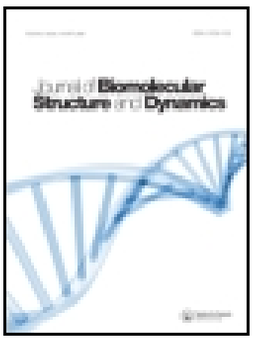

Taylor & Francis
Taylor & Francis Group

Journal of Biomolecular Structure and Dynamics

ISSN: (Print) (Online) Journal homepage: https://www.tandfonline.com/loi/tbsd20

Synthesis of new urease enzyme inhibitors as antiulcer drug and computational study

Muhammad Taha, Sukinah Ismail, Syahrul Imran, Noor Barak Almandil, Munther Alomari, Fazal Rahim, Nizam Uddin, Shawkat Hayat, Khalid Zaman, Mohamad Ibrahim, Bandar Alghanem, Imadul Islam, Rai Khalid Farooq, Mohamed Boudjelal & Khalid Mohammed Khan

To cite this article: Muhammad Taha, Sukinah Ismail, Syahrul Imran, Noor Barak Almandil, Munther Alomari, Fazal Rahim, Nizam Uddin, Shawkat Hayat, Khalid Zaman, Mohamad Ibrahim, Bandar Alghanem, Imadul Islam, Rai Khalid Farooq, Mohamed Boudjelal & Khalid Mohammed Khan (2021): Synthesis of new urease enzyme inhibitors as antiulcer drug and computational study, Journal of Biomolecular Structure and Dynamics, DOI: 10.1080/07391102.2021.1910072

To link to this article: https://doi.org/10.1080/07391102.2021.1910072

JOURNAL OF BIOMOLECULAR STRUCTURE AND DYNAMICS
https://doi.org/10.1080/07391102.2021.1910072

Taylor & Francis
Taylor & Francis Group

Synthesis of new urease enzyme inhibitors as antiulcer drug and computational study

Muhammad Taha[a], Sukinah Ismail[a,b], Syahrul Imran[c,d], Noor Barak Almandil[a], Munther Alomari[e], Fazal Rahim[f], Nizam Uddin[g], Shawkat Hayat[f], Khalid Zaman[f], Mohamad Ibrahim[a]*, Bandar Alghanem[h], Imadul Islam[h], Rai Khalid Farooq[i], Mohamed Boudjelal[h] and Khalid Mohammed Khan[j]

[a]Department of clinical pharmacy, Institute for Research and Medical Consultations (IRMC), Imam Abdulrahman Bin Faisal University, Dammam, Saudi Arabia; [b]College of clinical pharmacy, Imam Abdulrahman Bin Faisal University, Dammam, Saudi Arabia; [c]Atta-ur-Rahman Institute for Natural Product Discovery, Universiti Teknologi MARA (UiTM), Bandar Puncak Alam, Selangor, Malaysia; [d]Faculty of Applied Science, UiTM Shah Alam, Shah Alam, Selangor, Malaysia; [e]Department of Stem Cell Biology, Institute for Research and Medical Consultations (IRMC), Imam Abdulrahman Bin Faisal University, Dammam, Saudi Arabia; [f]Department of Chemistry, Hazara University, Mansehra, Khyber Pakhtunkhwa, Pakistan; [g]Department of Chemistry, University of Karachi, Karachi, Pakistan; [h]Medical Research Core Facility and Platforms (MRCFP, King Abdullah International Medical Research Center/King Saud bin Abdulaziz University for Health Sciences (KSAU-HS), King Abdulaziz Medical City (KAMC), NGHA, Riyadh, Saudi Arabia; [i]Department of Neuroscience Research, Institute for Research and Medical Consultations (IRMC), Imam Abdulrahman Bin Faisal University, Dammam, Saudi Arabia; [j]H. E. J. Research Institute of Chemistry, International Center for Chemical and Biological Sciences, University of Karachi, Karachi, Pakistan

Communicated by Ramaswamy H. Sarma

ABSTRACT

In search of potent urease inhibitor indole analogues (**1–22**) were synthesized and evaluated for their urease inhibitory potential. All analogues (**1–22**) showed a variable degree of inhibitory interaction potential having IC_{50} value ranging between 0.60 ± 0.05 to $30.90 \pm 0.90\,\mu M$ when compared with standard thiourea having IC_{50} value $21.86 \pm 0.90\,\mu M$. Among the synthesized analogues, the compounds **1, 2, 3, 5, 6, 8, 12, 14, 18, 20** and **22** having IC_{50} value 3.10 ± 0.10, 1.20 ± 0.10, 4.60 ± 0.10, 0.60 ± 0.05, 5.30 ± 0.20, 2.50 ± 0.10, 7.50 ± 0.20, 3.90 ± 0.10, 3.90 ± 0.10, 2.30 ± 0.05 and $0.90 \pm 0.05\,\mu M$ respectively were found many fold better than the standard thiourea. All other analogues showed better urease interaction inhibition. Structure activity relationship (SAR) has been established for all analogues containing different substituents on the phenyl ring. To understand the binding interaction of most active analogues with enzyme active site docking study were performed.

ARTICLE HISTORY
Received 14 December 2020
Accepted 23 March 2021

KEYWORDS
Urease inhibition; urease interaction with inhibitors; molecular docking

1. Introduction

Urease is an important nickel containing metalloenzyme that catalyse the hydrolysis of urea into ammonium and carbon dioxide (Krajewska, 2009). Often found in plants, fungi and bacteria play a pivotal role in nitrogen metabolism of plants during the germination process (Mobley et al., 1995). However, ammonia produced by urease can cause hepatic coma urolithiasis, hepatic encephalopathy, gastric and peptic ulcers in human (Li & Mobley, 2002; Mobley et al., 1995). Urease is known to cause virulence as well as determinant in pathogenicity of many human related diseases (Kwon-Chung et al., 2014). The urease activity of *Helicobacter pylori* at low pH in stomach plays a vital role in the pathogenesis of the gastric ulcers (Mobley, 1996). Therefore, urease inhibitors have been identified as first line to treatureolytic bacteria (Olivera-Severo et al., 2006). Due to this reason, urease inhibitors have special attention over the past decade and many compounds have been reported. Among those that had been reported includes disulphide derivatives (Khan et al., 2014), hydrazones (Taha et al., 2019), hydroxamic acids (Odake et al., 1994), and imidazoles like rabeprazole *etc* (ParkImamura & Kobashi, 1996).

In recent past, many papers had reported on urease inhibition by indole-based inhibitors (Naureen et al., 2015). A study conducted by Isaac *et. al* (Aslam et al., 2011). suggests that hydrazone derivatives were among the most active inhibitors of Jack bean urease that has been discovered. Some metal complexes of Sn (IV), Cu, Ni, Zn and Co with hydrazone have been reported as urease inhibitors (de Fátima et al., 2018).

Indole is nitrogen containing aromatic bicyclic planar molecule in which pyrrole ring is fused with benzene ring at 2 and 3 position. Indole ring are present in several natural products like fungal metabolites alkaloids and marine natural products. Numerous plants yielded indole like Jasmine (Bouchikhi et al., 2008; Douglass et al., 2011; Gribble, 2000)

CONTACT Muhammad Taha taha_hej@yahoo.com; mtaha@iau.edu.sa Department of clinical pharmacy, Institute for Research and Medical Consultations (IRMC), Imam Abdulrahman Bin Faisal University, P.O. Box 1982, Dammam 31441, Saudi Arabia
*Present address: Chemistry Department, Faculty of science, Assiut University, Assiut, Egypt

Supplemental data for this article can be accessed online at http://dx.doi.org/10.1080/07391102.2021.1910072

orange blossoms, citrus plants (AmirJaved & Kumar, 2008) and *Robiniapseudacacia* (Van Order & Lindwall, 1942).

In animal body it also presents in brain (Dharmendra et al., 2010), bile (Lucas et al., 1985), in pancreas, liver (Pandeya et al., 1998), and where pus formation occurs (Siddiqui et al., 2008) and found in coal tar (Omar et al., 1996). Indole ring system is a valuable structural moiety with a broad spectrum biological activities including antifungal (Przheval'skii et al., 1997), antioxidant (Poeggeler et al., 1993), antimicrobial (Hiari et al., 2006), anticonvulsant (Ali et al., 2013), anti-HIV (SuzenBuyukbingol, 1998), plant growth regulator (Karadeniz et al., 2011), antihistaminic (Battaglia et al., 1999), anticancer (Chen et al., 1996), analgesic and anti-inflammatory (Guerra et al., 2011). The N'-benzylidene-2-(1H-indol-3-yl)acetohydrazide showed cytotoxic, antimicrobial activities (Choppara et al., 2019), thymidine phosphorylase (Taha et al., 2020), FAK inhibition (Kassab & Hassan, 2018), COX-2 inhibitors (de Oliveira Moraes et al., 2018; Sharma et al., 2019), Dual IGF-1R/SRC inhibitors (Schmidt et al., 2011), selective novel tubulin inhibitors (Tantak et al., 2017), and cyclooxygenase inhibitor (Wani et al., 2019).

We are working on new inhibitors for urease and in recent past we have reported different classes of compound against urease inhibition (Alomari et al., 2019; Seraj et al., 2021; Wahid et al., 2020; Zaman et al., 2019) (Figure 1). We synthesized indole derivatives which are not directly attached with the ring. The most of inhibitors reported having aromatic ring directly attached with other functional. The acetyl chain which will give the free movement to the other part of the molecules and will give better results.

2. Result and discussion

2.1. Chemistry

Indole derivatives were synthesized by refluxing methyl 2-(1*H*-indol-3-yl)acetate with hydrazine hydrate in methanol for 6 hrs yielded 2-(1*H*-indol-3-yl)acetohydrazide as intermediate product (I). The intermediate product (I) was recrystallized using methanol. 2-(1*H*-indol-3-yl)acetohydrazide was then treated with varied aldehyde (**1–22**) (Table 1) in methanol for 3–4 hrs yielded indole derivatives (**1–22**) (Scheme 1). The reaction completion was monitored using thing layer chromatography (TLC). The crude product was recrystallized in methanol to yield pure compounds (**1–22**). The compounds **1**, **2**, **4**, **6**, **7**, **10**, **11–13**, **17**, **18**, **20** and **22** are reported earlier (Hanna et al., 2007; Ju et al., 2019; Liu et al., 2019; Mirfazli et al., 2016). The compounds **3**, **5**, **8**, **9**, **14**, **15**, **16**, **19** and **21** are new and all scaffold are reported for urease activity first time.

2.2. In vitro urease interaction study with inhibitors

Our research group is continuously working to explore potent bioactive compounds (Ali et al., 2018; Saify et al., 2014; Taha et al., 2015; 2015; Taha & Wadood, 2018). In current study we have synthesized a new class of indole analogues (**1–22**) and their urease inhibitory potential were evaluated. All synthesized compounds exhibited a variable degree of inhibitory potential having IC_{50} value ranging between 0.60 ± 0.05 to $30.90 \pm 0.90\,\mu M$ when compared with standard thiourea having IC_{50} value $21.86 \pm 0.90\,\mu M$. Among the synthesized analogues, compounds **1, 2, 3, 5, 6, 8, 12, 14, 18, 20** and **22** having IC_{50} value 3.10 ± 0.10, 1.20 ± 0.10, 4.60 ± 0.10, 0.60 ± 0.05, 5.30 ± 0.20, 2.50 ± 0.10, 7.50 ± 0.20, 3.90 ± 0.10, 3.90 ± 0.10, 2.30 ± 0.05 and $0.90 \pm 0.05\,\mu M$ were found many folds better than the standard thiourea. All other analogues showed better urease inhibition. Structure activity relationships are primarily based on substituted phenyl ring.

The most potent analogue among the synthesized analogues is compound **5** ($IC_{50} = 0.60 \pm 0.05\,\mu M$) having 3, 4-dihydroxy substitution on one of the phenyl rings. The greater inhibition shown by this scaffold may be due to the presence of OH moiety on one of the phenyl rings which is possibly involved in hydrogen bonding.

If we compare compound **5** with other dihydroxy substituted analogues like compound **2** ($IC_{50} = 1.20 \pm 0.10\,\mu M$) having hydroxyl moiety present at position2and 4 on the phenyl ring, compound **3** ($IC_{50} = 4.60 \pm 0.10\,\mu M$)having hydroxyl moiety present at position3 and 5 on the phenyl ring, compound **6** ($IC_{50} = 5.30 \pm 0.20\,\mu M$) having hydroxyl moiety present at position2 and 5 on the phenyl ring and compound **22** ($IC_{50} = 0.90 \pm 0.05\,\mu M$) having hydroxyl moiety present at position 2and 3 on the phenyl ring. The difference in the potential of these analogues seems due to varied position of substituent on phenyl ring (Figure 2).

Comparison of compound **5** ($IC_{50} = 0.60 \pm 0.05\,\mu M$) with compound **20** ($IC_{50} = 5.30 \pm 0.20\,\mu M$) showed that replacing a hydroxyl group with a methoxy group decrease the activity to 10 folds which is an indication that intermolecular hydrogen bonding is a significant factor for enzyme inhibition. Furthermore, when compound **2** ($IC_{50} = 1.20 \pm 0.10\,\mu M$) was compared with compound **21** ($IC_{50} = 30.90 \pm 0.90\,\mu M$) having methoxy group at position 2 and 4 instead of hydroxyl group decreases its activity to 26 folds which suggests us that the hydroxyl group play a key role in activity. Comparison of compound **2** with compound **8,** showed a very interesting result ($IC_{50} = 2.50 \pm 0.10\,\mu M$) that adding more hydroxyl group to compound **2** also decreases its activity hence position and numbers of hydroxyl play the key role in activity (Figure 2).

Similarly by comparing scaffold **1**($IC_{50} = 3.10 \pm 0.10\,\mu M$) possess nitro group at position 4 of the phenyl ring with scaffold **10** ($IC_{50} = 12.30 \pm 0.30\,\mu M$) having nitro group at position 2 of phenyl ring and scaffold **11**($IC_{50} = 12.20 \pm 0.30\,\mu M$) having nitro group at position 3 of phenyl ring. The slight difference was observed in the potential of these three-scaffolds, which may be due to the interaction with enzyme (Figure 3).

Similarly, by comparing analogue **13** ($IC_{50} = 17.40 \pm 0.40\,\mu M$) having 4-chloro substitution on phenyl ring with analogue **17** ($IC_{50} = 12.20 \pm 0.30\,\mu M$) having 3-chloro substitution on phenyl ring. The little bit difference was observed in the potential of these two analogues may be due to way of interaction with enzyme (Figure 4).

Table 1. *In vitro* urease inhibitory activity of compounds (**1–22**).

S. NO	R	IC_{50} ± SEM[a]	S#	R	IC_{50} ± SEM[a]
1	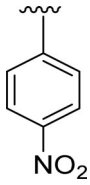	3.10 ± 0.10	**12**	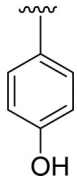	7.50 ± 0.20
2	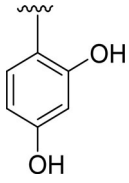	1.20 ± 0.10	**13**	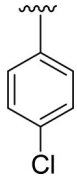	17.40 ± 0.40
3	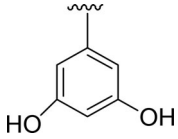	4.60 ± 0.10	**14**	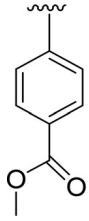	3.90 ± 0.10
4	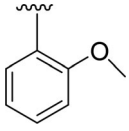	16.60 ± 0.20	**15**	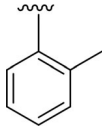	26.20 ± 0.60
5	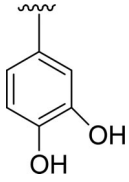	0.60 ± 0.05	**16**	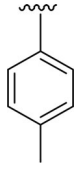	18.20 ± 0.50
6	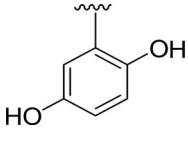	5.30 ± 0.20	**17**	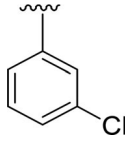	12.20 ± 0.30
7	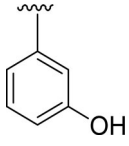	13.70 ± 0.40	**18**	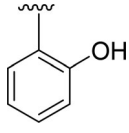	5.90 ± 0.10
8	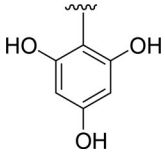	2.50 ± 0.10	**19**	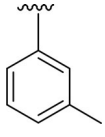	20.90 ± 0.50
9	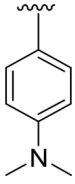	11.10 ± 0.30	**20**	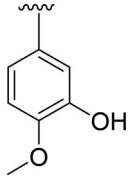	2.30 ± 0.05

(*continued*)

Table 1. Continued.

S. NO	R	IC_{50} ± SEM[a]	S#	R	IC_{50} ± SEM[a]
10	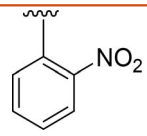	12.30 ± 0.30	**21**	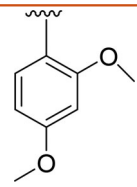	30.90 ± 0.90
11	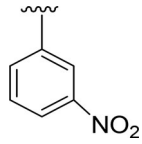	12.20 ± 0.30	**22**	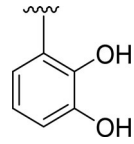	0.90 ± 0.05
Standard Thiourea			21.86 ± 0.40		

By comparing compound **15** (IC_{50} = 26.20 ± 0.60 μM) having 2-methyl substitution on phenyl ring with compound **16** (IC_{50} = 18.20 ± 0.50 μM) having 4-methyl substitution on phenyl ring and compound **19** (IC_{50} = 20.90 ± 0.50 μM) having 3-methyl substitution on phenyl ring. The observed difference in potential among these analogues may be due to way of interaction with active side of enzyme in a different way (Figure 5).

The analogues **7** (IC_{50} = 13.70 ± 0.40 μM), **12** (IC_{50} = 7.50 ± 0.20 μM) and **18** (IC_{50} = 5.90 ± 0.10 μM) having monohydroxy at position 3, 4, 2 respectively. The most active among them is **18** which may be due to better fit with the enzyme active as compared to other analogues **7** and **8** but still the compound **12** also showed a better activity then compound **7** may be due to same reason. If we compare compound **18** with the compound **4** (IC_{50} = 16.60 ± 0.20 μM) which is 2-methoxy instead of 2-hydroxy its activity dropped two-folds which may be due to the possible hydrogen bonding ability of compound **18** with enzyme (Figure 6).

The compound **9** (IC_{50} = 11.10 ± 0.30 μM) having dimethylamine showed good activity this may be due to good interaction with enzyme. On the other hand, compound **14** (IC_{50} = 3.90 ± 0.10 μM) showed potent activity having ester moiety at position 4 this may be enzyme active side interaction with ester (Figure 7).

In the above study it was observed that position, nature and number of substituents on phenyl ring greatly affected the inhibition of the synthesized analogues. To further explore the binding interaction of most active analogues with active site of enzyme, molecular docking study was performed.

2.3. Computational study of interaction of urease enzyme with most active inhibitors

All compounds were docked into the binding cavity of urease enzyme (PDB ID: 4ubp). The results showed that active compounds **2**, **5**, and **22** can fit well in the urease binding

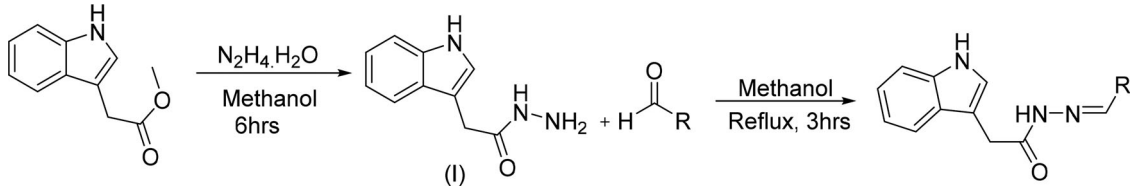

Scheme 1. Synthesis of indole derivatives (**1–22**)

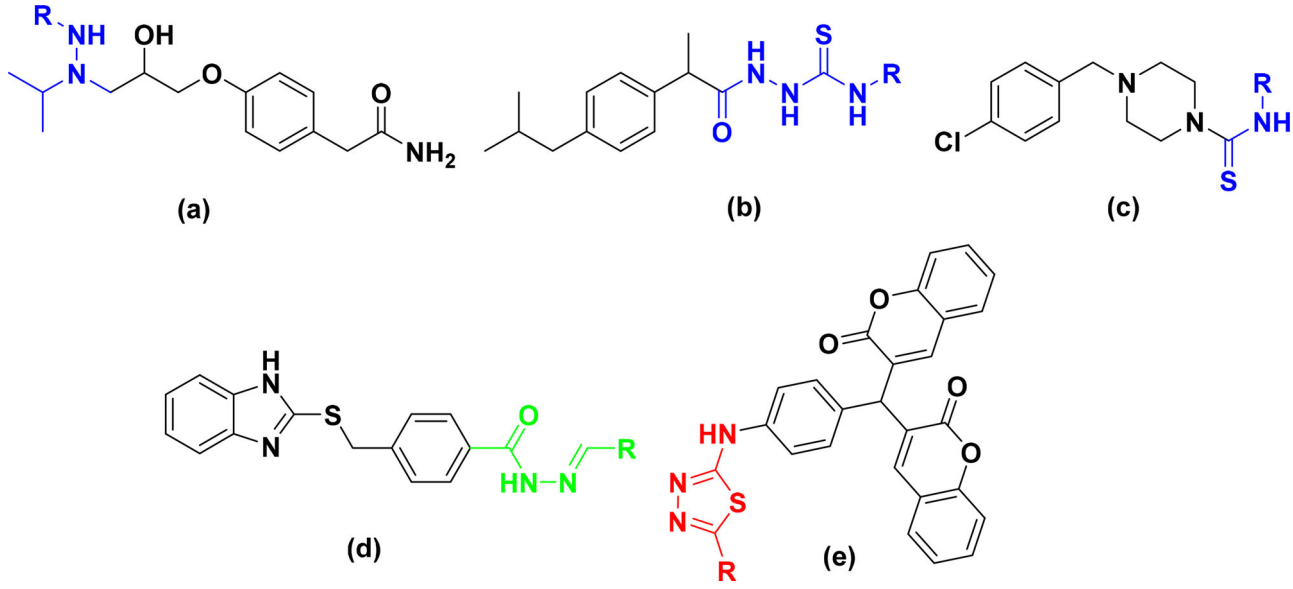

Figure 1. In recent past we published few urease inhibitors (**a–e**).

cavity. Binding affinity, residues involved, interactions, and distance of ligand-residue interactions obtained from the docking results for selected compounds are summarized in Table 2.

The most potent compound **5** (IC_{50} = 0.60 ± 0.05) showed good interactions pattern as shown in (Figure 8). The hydroxyl groups in compound **5** which are located at *meta* and *para* positions over the aromatic ring of the benzylidene moiety. The docking results revealed that hydroxyl group at *para* position of the benzylidene moiety was observed to act as an acceptor and interact with nickel ion (NI798) at 3.2 Å thus retarding the catalytic activity of urease. The same hydroxyl group also acts a hydrogen bond donor that forms interaction with oxygen on the side chain (OD2) of nickel-binding residue Asp363 at 1.8 Å. The benzylidene ring interactions were stabilized by an electrostatic π-cation interaction with NH_2 on the guanidine moiety of Arg339. Another interaction of hydrogen bonding was observed between the NH of the hydrazine linkage and imidazole on the side chain of catalytic residue His323 which takes place through a π-donor hydrogen bond at a distance of 2.7 Å. As a result, the interaction of compound **5** with Arg339 and catalytic residue His323 had also influenced the decrease in catalytic activity of urease enzyme. Other interaction includes indole ring being stabilized by two hydrophobic π-alkyl interactions with the side chain (C) of Lys169 (Figure 8).

Docking results for compound **22**, the hydroxyl at *meta* position of the benzylidene moiety acts as an acceptor to interact with the nickel ion (NI798) with the cavity of urease enzyme. The hydroxyl group at *meta* position also forms a further interaction with the oxygen on the side chain of nickel-binding residue Asp363.Hydroxyl group at the *ortho* position of benzylidene ring forms a hydrogen bonding with nitrogen on the imidazole ring of His222 at 1.8 Å. The NH of hydrazone linkage forms a hydrogen bonding with the side chain (OD2) of Asp224 at 1.7 Å. The benzylidene ring for compound **22** is sandwiched between two hydrophobic π-alkyl interactions involving the backbone (C) of both Ala366 and guanidine moiety Arg339 while indole is stabilized by two hydrophobic π-alkyl interactions with the backbone of Ala170 (Figure 9).

Compound **2** which is the third most active displayed form a metal interaction through hydroxyl at *para* position of the benzylidene moiety with nickel ion(NI798) at 2.1 Å. It was also found to form a hydrogen bonding with oxygen (OD2) on the backbone of nickel-binding residue Asp363 at a distance of 2.9 Å. Furthermore, the other hydroxyl group at *ortho* position forms a hydrogen bonding with the nitrogen (Nε2) on the imidazole moiety of catalytic residue His323 at a distance of 3.0 Å. Another hydrogen bonding was observed between NH of the hydrazone linkage and oxygen on the backbone of residue Cys322 present in the catalytic core of the enzyme at a distance of 2.8 Å. The results also showed that Cys322 stabilizes the aromatic ring on indole through hydrophobic π-alkyl interaction. Another hydrophobic π-alkyl interaction was observed between Lys169 and aromatic ring of indole moiety (Figure 10).

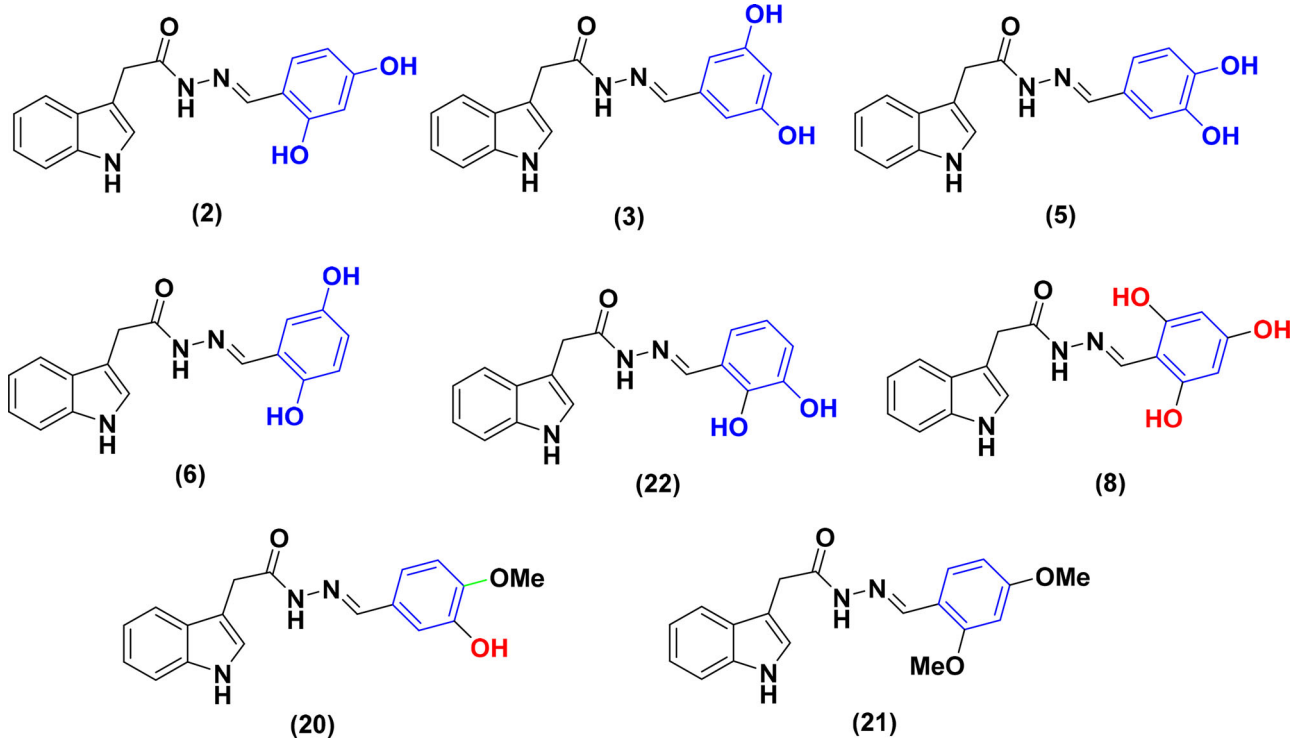

Figure 2. Dihydroxy, trihydroxy and dimethoxy substituted analogues.

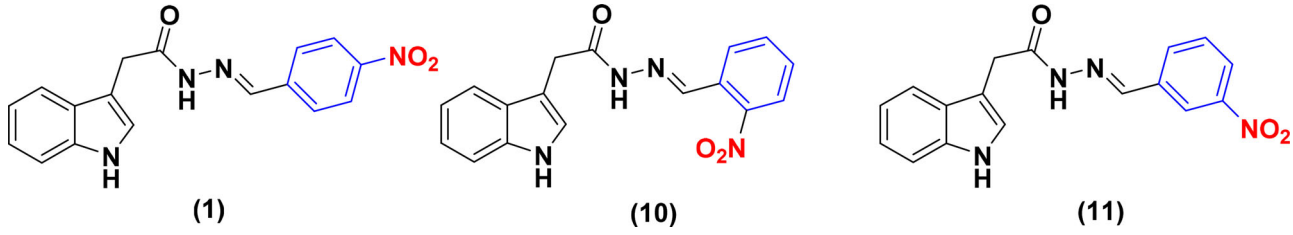

Figure 3. Nitro substituted analogues**1**, **10** and **11**.

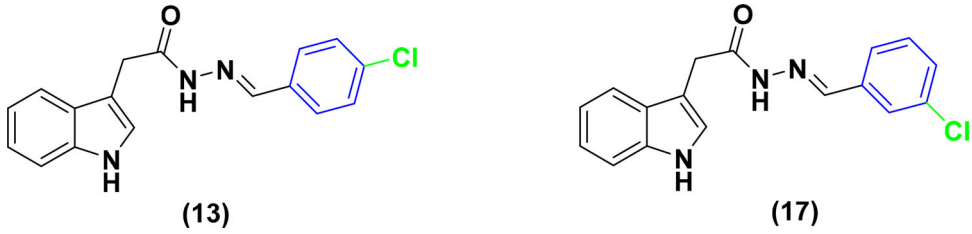

Figure 4. Chloro substituted analogues **13** and **17**.

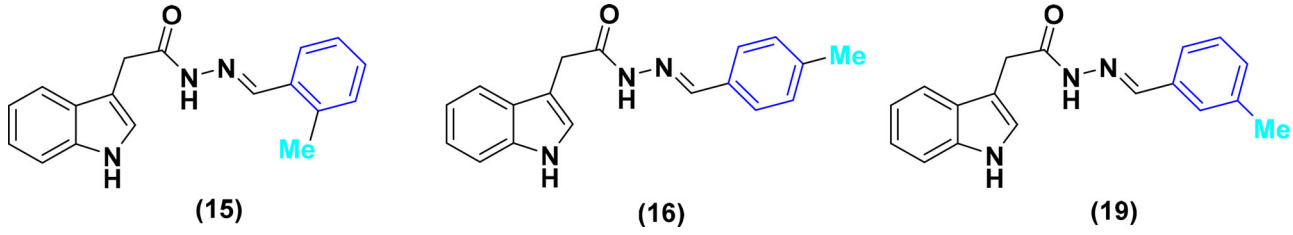

Figure 5. Methyl substituted analogues **15**, **16** and **19**.

Docking studies had been used to further visualize the importance of substituents (R) of each compound and how these substituents affect the activity. Comparison between compounds **12**, **2**, and **5** showed the significance of hydroxyl substituents with reference to their position on the ring. Based on the docking results in Figure 11, compound **12** that is the least active among these 3 compounds was observed to form minimum interaction in the active site as compare to the other 2 compounds. Compound **12** displayed a single interaction with nickel ion, while compounds **2** and **5** demonstrated the

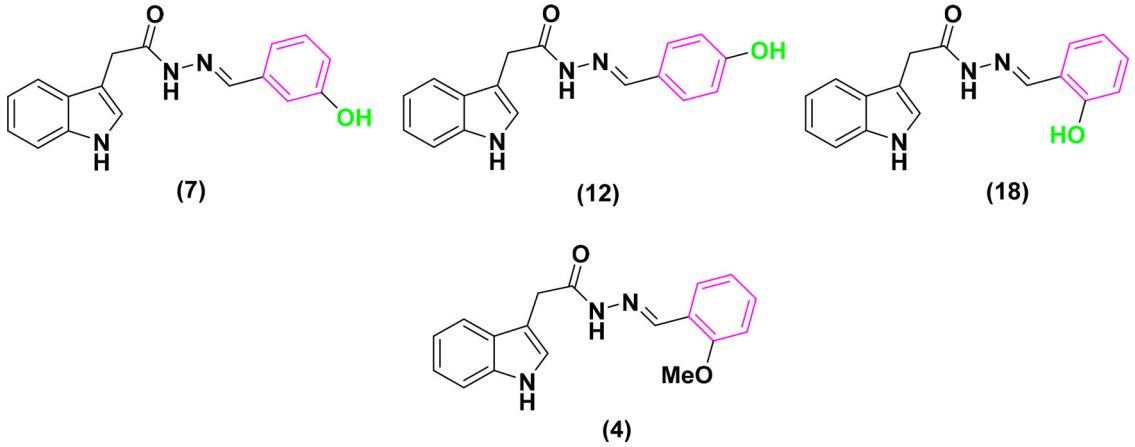

Figure 6. Monohydroxy substituted analogues **15**, **16** and **19**and methoxy analogue **4**.

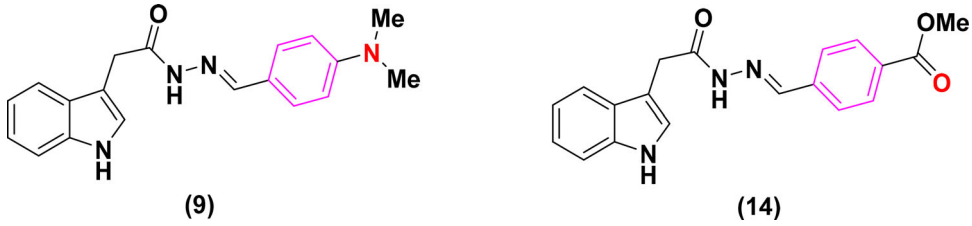

Figure 7. Ester and amino substituted analogues **9** and **14**.

Table 2. Binding affinity, residues involved, interactions, and distance of ligand-residue interactions.

Comp. No.	IC_{50} (μM)	Binding affinity (kcal/mol)	Residues	Interaction	Distance (Å)
5	0.6	−11.8	NI798	Metal acceptor	3.2
			Asp363	Hydrogen bond	1.8
			His323	Hydrogen bond	2.7
22	0.9	−10.7	NI798	Metal acceptor	3.5
			Asp363	Hydrogen bond	1.9
			His222	Hydrogen bond	1.8
			Asp224	Hydrogen bond	1.7
2	1.2	−10.5	NI798	Metal acceptor	2.1
			Asp363	Hydrogen bond	2.9
			His323	Hydrogen bond	3.0
			Cys322	Hydrogen bond	2.8
20	2.3	−10.2	Ni798	Metal acceptor	4.3
			Asp224	Hydrogen bond	2.3
1	3.1	−10.3	Ni798	Metal acceptor	2.7
			His249	Electrostatic	2.3
			Cys322	Hydrogen bond	2.8
			Glu166	Hydrogen bond	3.1
18	5.9	−9.8	Ni798	Metal acceptor	3.5
			His222	Hydrogen bond	2.3
			Asp224	Hydrogen bond	2.5
12	7.5	−9.6	Ni798	Metal acceptor	3.5
			Asp363	Hydrogen bond	2.5
			His249	Hydrogen bond	2.6
			Cys322	Hydrogen bond	2.9
9	11.1	−9.3	Cys322	Hydrogen bond	2.4
11	12.2	−9.4	Ni798	Metal acceptor	3.4
10	12.3	−9.4	Ni798	Metal acceptor	3.7
4	16.6	−9.4	Ni798	Metal acceptor	5.6
21	30.9	−8.0	Cys322	Hydrogen bond	2.8

ability to form multiple metal-acceptor interactions with nickel ion as well as hydrogen bonding with the enzyme active residues like Asp363 and His323. It is very important for the hydroxyl to be able to interact well with nickel ion as well as residues within the active site.

Moving on further with the activity relationship of hydroxyl substituents towards the inhibition activity, docking results of compounds **2**, **4**, **5**, **12**, **18**, **20**, and **21** are being compared. The results showed in Figure 12 explain how protecting hydroxyl group affect the activity. Compound **20**, which is a derivative of compound **5**, displayed significant reduction in activity, signifying effect of converting hydroxyl group at *para* position to methoxy. Comparison between docking results of compound **5** and **20** (Figure 12) showed that methoxy at *para* position is not able to interact well with nickel ion over a distance apart due to steric factor.

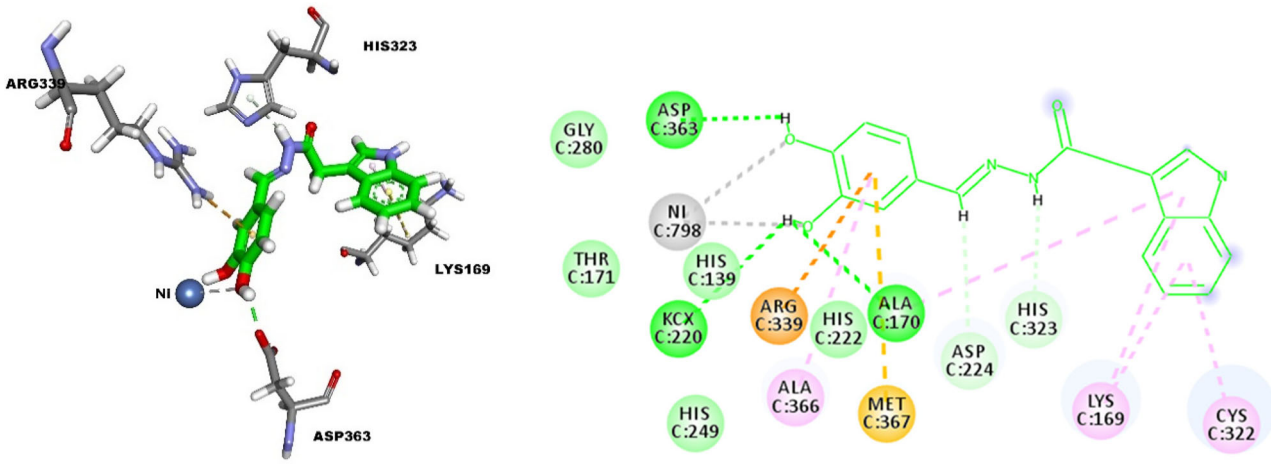

Figure 8. Molecular docking and 2D interaction diagram for compound **5** with urease enzyme (4UBP).

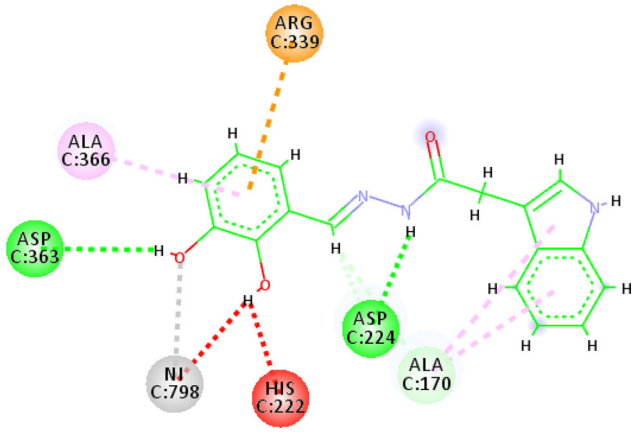

Figure 9. Molecular docking and 2D interaction diagram for compound **22** with urease enzyme (4UBP).

Similar observation for compound **2** and **21**, in which both hydroxyl groups of compounds **2** were being converted into methoxy group, causing the great activity loss. Docking results displayed that presence of two methoxy groups causes much steric hindrance thus preventing the methoxy substituents from interacting with nickel ion. Another similar observation was compounds **4** and **18**. Compound **4** which possess a methoxy substituent at *ortho* position displayed less inhibition compared to compound **18** with hydroxyl group at the same position. Investigating these further using docking results showed that compound **4** is not able to fit in well in the cavity and has formed significantly less interaction with active site.

As for compounds with nitro substituents, compounds **1**, **10**, and **11**, docking results suggest that the activity is mainly due to the ability of nitro substituents to form interaction with nickel ion, besides the other residue in the cavity (Figure 13). Compound **1** that has nitro substituent at position is able to interact well within the binding site due to its linear shape, which allows the nitro substituent to be positioned deep in the cavity and close to the nickel ion. It was also well observed that compounds **10** and **11**, having nitro substituent at *ortho* and *meta* position losses their ability to inhibit urease activity, as nitro substituent at *ortho* and meta positions tend to be too bulky to allow the aromatic ring to be positioned properly within the active site, thus allowing nitro substituent to interaction with nickel ion, as can be seen for compound **1**. The importance of oxygen on nitro substituent as metal-acceptor can also be seen through interaction of compound **9**, in which the oxygen atoms are now replaced with two methyl groups and this has resulted in decrease of inhibition activity.

2.4. In silico ADMET analysis

Most of drug failures at early and late pipeline occur due to undesired pharmacokinetics and toxicity problems. If these issues could be addressed early, it would be extremely advantageous for the drug discovery process.

In silico ADMET analysis was conducted to predict the pharmacokinetic properties of the compounds and address undesired pharmacokinetics and toxicity problems. The compounds were evaluated for various parameters like aqueous solubility, blood brain barrier (BBB) penetration, CYP2D6 binding, hepatotoxicity, human intestinal absorption (HIA), and plasma protein binding. Overall observation on the ADMET biplot showed that all compounds are predicted to be within the ellipses of HIA and BBB (Figure 14). It is expected that more than 90% of all compounds will be absorbed into the bloodstream. This is based on the results that showed all compounds are well within the absorption level for both 95 and 99% confidence ellipses. The results in Table 3 indicates that all compounds have very good HIA level 0. For blood brain barrier (BBB), all compounds are within the 99% confidence ellipse except for compound **8**. On the other hand, only 13 compounds are within the BBB 95% confidence ellipse.

Table 3 shows a detailed prediction that majority of the compounds have high to low BBB penetration levels (levels 1–3) except for compounds **8** which could not penetrate the blood brain barrier (Level 4). Compounds **13**, **15**, **16**, **17**, and **19** are high BBB penetrants (level 1) while compounds **4**, **9**, and **21** displayed medium BBB penetration (level 2). The rest of the compounds displayed low BBB penetration (level 3). As for the aqueous solubility, all compounds were predicted to have moderate and good aqueous solubility level (2 and 3).

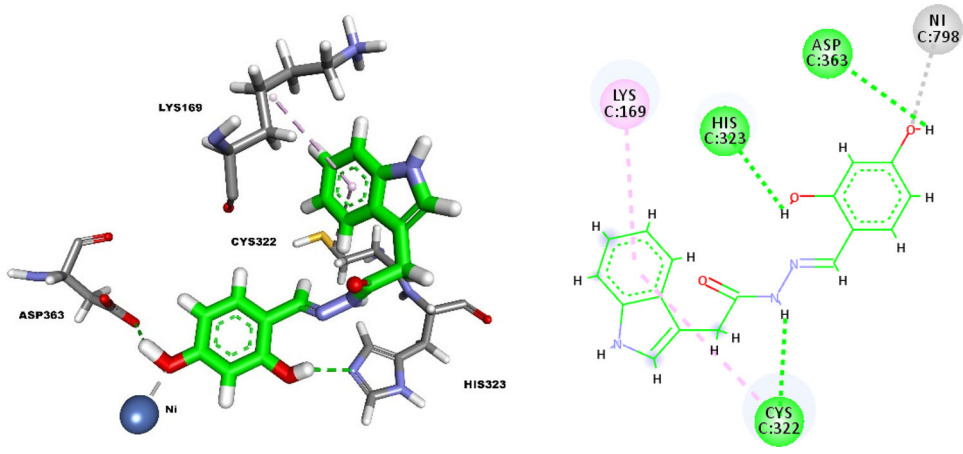

Figure 10. Molecular docking and 2D interaction diagram for compound **2** with urease enzyme (4UBP).

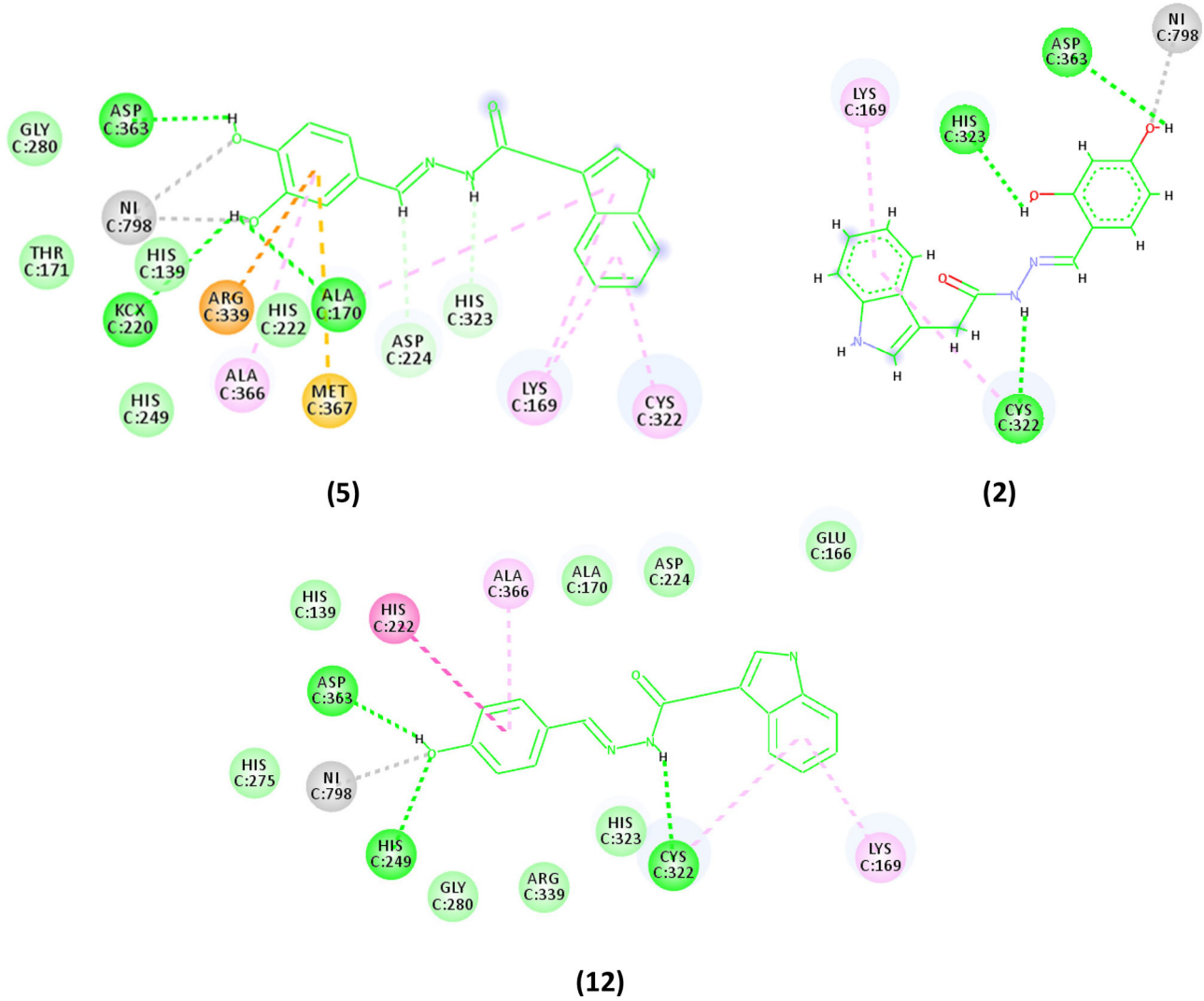

Figure 11. The 2D interaction diagram of compounds **2**, **5** and **12** displaying binding position and interaction with nickel ion and residues within the active site of urease enzyme.

Prediction indicate that all compounds are hepatotoxic (level 1, Table 3) and therefore requires extra precaution. On the other hand, all compounds are noninhibitors of CYP2D6 and this suggests that these compounds are well metabolized in Phase-I metabolism. Finally, the ADMET plasma protein binding property prediction showed that 7 compounds displayed the ability to bind to protein plasma (**9**, **10**, **13**, **15**, **16**, **17**). On contrary, prediction for other compounds suggests that they will not bind to protein plasma. Observations suggest that active compounds **2**, **5**, **22** have

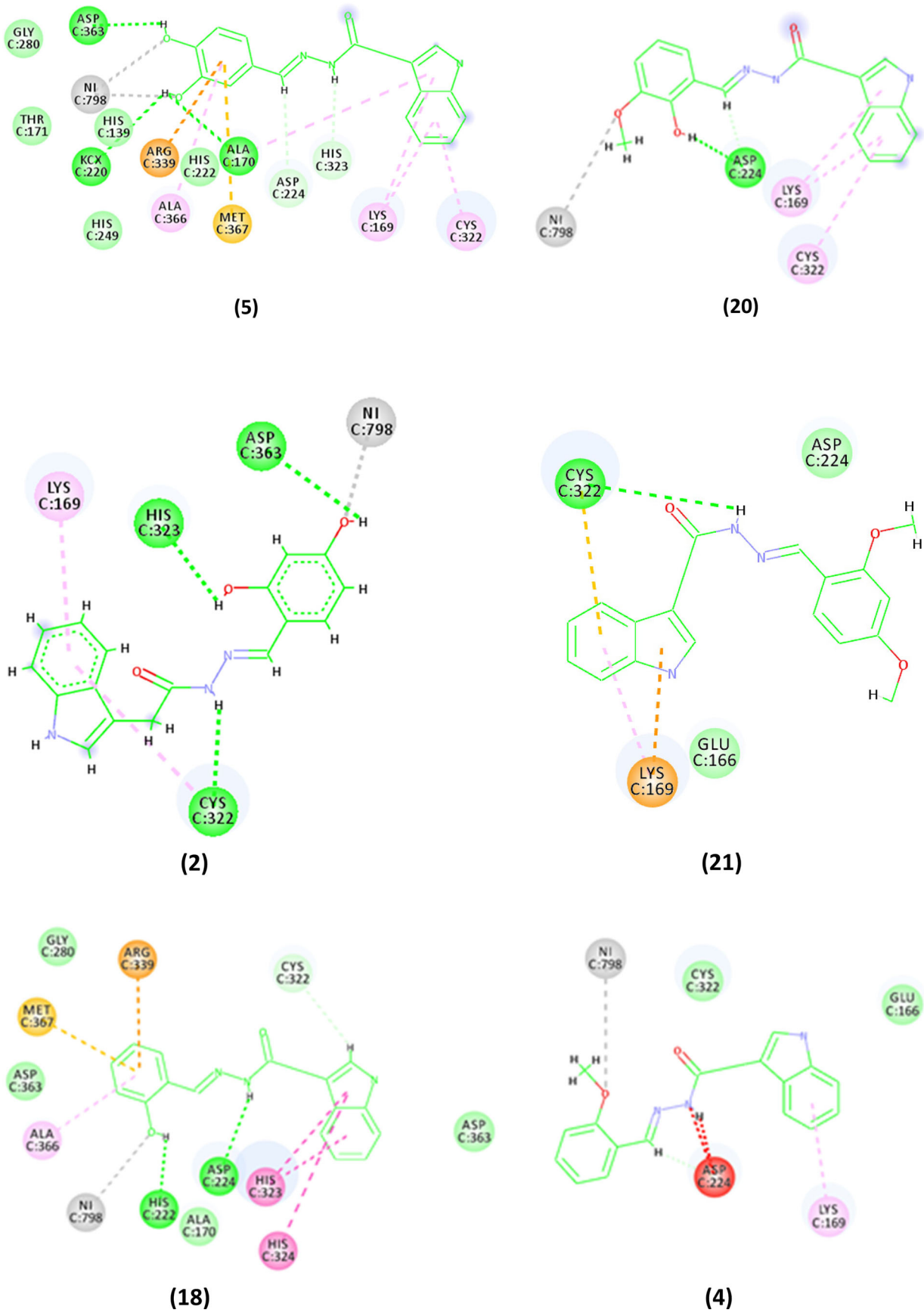

Figure 12. The 2D interaction diagram of compounds **2**, **4**, **5**, **18**, **20** and **21** displaying effect of protecting hydroxyl group on interaction with nickel ion and important residues within the active site of urease enzyme.

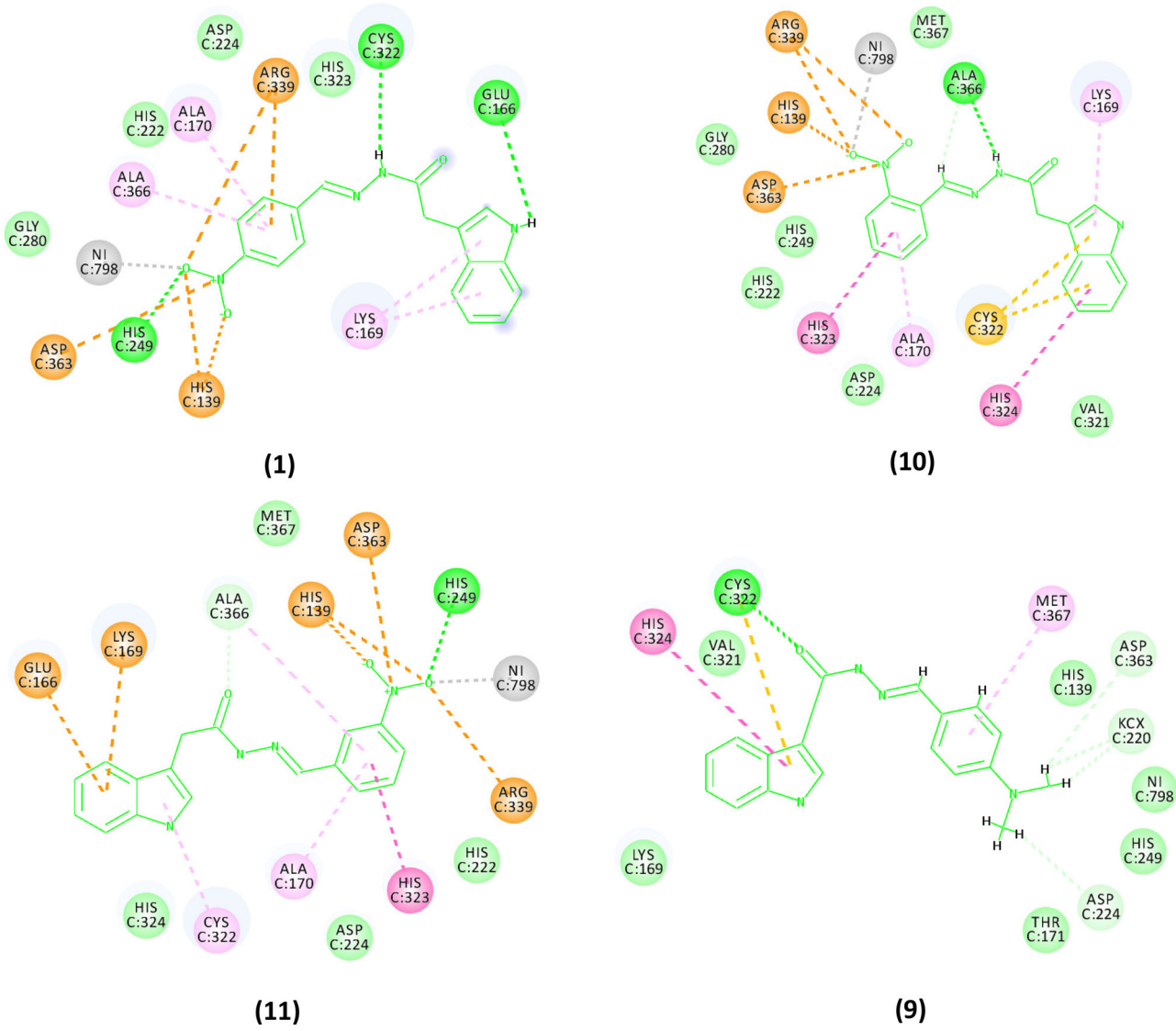

Figure 13. Interaction of compounds **1**, **9**, **10** and **11** that are bearing nitro and amino substituents within the active site of urease enzyme.

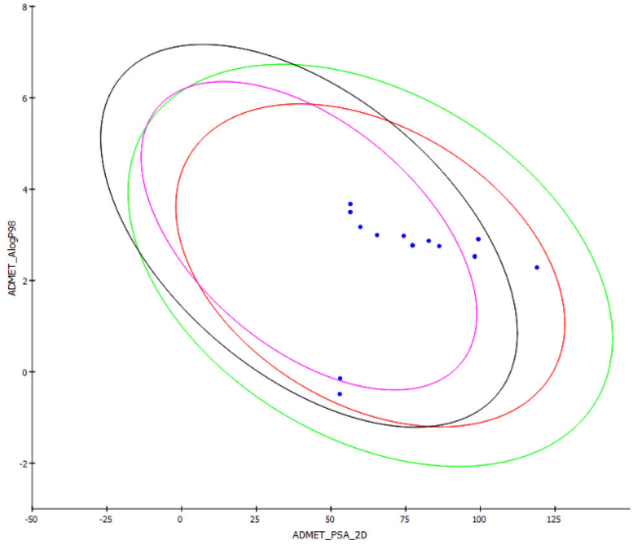

Figure 14. ADMET plot for all compounds against Absorption 95% (Red), Absorption 98% (Yellow), Blood Brain Barrier 95% (Blue), and Blood Brain Barrier 98% (Black).

high potential. Through the *in silico* ADMET analysis compounds **2**, **5** and **22** was found have good solubility in aqueous solution and high intestinal absorptivity. These compounds are also noninhibitors of CYP2D6 and they do not interfere with drug metabolism process taking place in the liver. Their ability not to bind to protein plasma indicates good bioavailability and are not likely to be highly bound to carrier proteins in the blood. However, these compounds need to be further evaluated for their low BBB penetration and hepatoxicity.

3. Assay protocol

The reaction mixtures containing solution of 25 µL of enzyme (jack bean urease) and 55 µL of buffer at pH 6.8, having 100 mM urea, were incubated with 5 µL of test compounds concentration (from 0.5 to 0.00625 mM) for 15 min at 30 °C in 96-well plates. Urea concentration were changed from 2 to 25 mM for assessment. Urease activity was determined by

Table 3. ADMET prediction of 22 synthesized indole derivatives.

Comp. No.	Solubility level[a]	BBB level[b]	Absorption level[c]	CYP2D6 prediction[d]	Hepatotoxic prediction	PPB prediction[e]
1	2	3	High	Non-inhibitor	Toxic	FALSE
2	3	3	High	Non-inhibitor	Toxic	FALSE
3	3	3	High	Non-inhibitor	Toxic	FALSE
4	2	2	High	Non-inhibitor	Toxic	FALSE
5	3	3	High	Non-inhibitor	Toxic	FALSE
6	3	3	High	Non-inhibitor	Toxic	FALSE
7	3	3	High	Non-inhibitor	Toxic	FALSE
8	3	4	High	Non-inhibitor	Toxic	FALSE
9	2	2	High	Non-inhibitor	Toxic	TRUE
10	2	3	High	Non-inhibitor	Toxic	TRUE
11	2	3	High	Non-inhibitor	Toxic	FALSE
12	3	3	High	Non-inhibitor	Toxic	FALSE
13	2	1	High	Non-inhibitor	Toxic	TRUE
14	2	3	High	Non-inhibitor	Toxic	FALSE
15	2	1	High	Non-inhibitor	Toxic	TRUE
16	2	1	High	Non-inhibitor	Toxic	TRUE
17	2	1	High	Non-inhibitor	Toxic	TRUE
18	3	3	High	Non-inhibitor	Toxic	FALSE
19	2	1	High	Non-inhibitor	Toxic	TRUE
20	3	3	High	Non-inhibitor	Toxic	FALSE
21	2	2	High	Non-inhibitor	Toxic	FALSE
22	3	3	High	Non-inhibitor	Toxic	FALSE

[a]Solubility of compounds in aqueous solution (2= Moderate, 3 = High).
[b]Blood brain barrier penetration level (1= Good, 2 = Moderate, 3 = Low, 4= No penetration).
[c]Human intestinal absorptivity level.
[d]Ability of compounds to inhibit CYP2D6.
[e]Ability of compounds to bind to protein plasma.

measuring ammonia production using the indophenol method as described by Weatherburn. Briefly 70 μL of alkali reagent (0.5%w/v NaOH and 0.1% active chloride NaOCl) and 45 μL of phenol reagent (1% w/v phenol and 0.005% w/v sodium nitroprusside) were added to each other well. After 50 min increasing absorbance at 630 nm was measured, using microplate reader (Molecular device, USA). All reactions were performed in triplicate in a final volume of 200 μL. The results (change in absorbance per min) were processed by using software Soft Max Pro (molecular device, USA). Entire assay was performed at PH 6.8. percent inhibition was calculated from the formula below.

$$\% \text{ inhibition} = 100 - (OD_{test}/OD_{control}) \times 100.$$

Thiourea was used as standard inhibitor for urease (Wani et al., 2019).

4. Material and method

4.1. General experiment

Nuclear Magnetic Resonance (NMR) analysis was performed on JNM – ECS 400 MHz spectrometer. High Resolution Electron Impact Mass Spectra (HREI-MS) were carried on Finnigan MAT-311A (Germany) mass spectrometer. Precoated silica gel aluminium plates (Kieselgel 60, 254, Merck, Germany) were used for Thin Layer Chromatography (TLC). Ultraviolet Visible (UV) spectroscopy was conceded to visualize the chromatogram at 254 and 365 nm.

4.2. General procedure for the synthesis of indole derivatives (1–22)

Indole derivatives were synthesized by refluxing methyl 2-(1*H*-indol-3-yl) acetate (5 mmol) with hydrazine hydrate (5 mL) in methanol (15 mL) for 6 hrs yielded 2-(1*H*-indol-3-yl)acetohydrazide as intermediate product (I). The completion of reaction was monitored using TLC. The excess solvent were evaporated under vacuum to obtain the crude product and recrystallized in methanol to obtained pure product. Equimolar intermediate product (I) then further treated with different aldehydes (**1–22**) in methanol (15 mL) for 3–4 hrs in the presence of catalytic amount of acetic acid yielded indole derivatives (**1–22**). The completion of reaction was monitored with the help of TLC. The crude was then recrystallized in methanol to obtained pure product (Hanna et al., 2007; Ju et al., 2019; Liu et al., 2019; Mirfazli et al., 2016).

4.3. 2-(1h-indol-3-yl)-N′-(4-nitrobenzylidene)acetohydrazide (1)

Yield: (88%); mp 289–291 °C match (Hanna et al., 2007; Ju et al., 2019; Liu et al., 2019; Mirfazli et al., 2016); ^{1}HNMR; (400 MHz, DMSO-d_6): δ 11.70 (s, 1H, NH), 11.52 (s, 1H, NH), 8.70 (s, 1H), 8.36 (d, 2H, J = 8.0 Hz), 7.89 (d, 2H, J = 8.0 Hz), 7.60 (t, 1H, J = 7.0 Hz), 7.22 (d, 1H, J = 7.5 Hz), 6.92–6.86 (m, 3H), 3.69 (s, 2H, CH_2);^{13}CNMR (100, MHz, DMSO) δ 171.0,150.5, 144.3, 139.5, 136.3, 127.2, 125.0, 125.0, 124.2, 124.2, 123.5, 121.4, 119.5,118.6, 111.2, 109.5, 36.0, HR-EIMS *m/z*, calcd for $C_{17}H_{14}N_4O_3$ $[M]^+$ 322.1066 found 322.1053.

4.4. N′-(2,4-dihydroxybenzylidene)-2-(1H-indol-3-yl)acetohydrazide (2)

Yield: (89%); mp 279–281 °C match (Hanna et al., 2007; Ju et al., 2019; Liu et al., 2019; Mirfazli et al., 2016); ^{1}HNMR (400 MHz, DMSO-d_6): δ 11.62 (s, 1H, NH), 11.28 (s, 1H, NH), 11.28 (s, 2H, OH), 7.75 (m, 1H), 7.34 (t, 2H, J = 7.0 Hz), 7.22 (d, 2H, J = 7.5 Hz), 6.92–6.86 (m, 2H), 3.39 (s, 2H, CH_2);^{13}CNMR

(100, MHz, DMSO) δ 171.0, 162.1, 162.1, 146.2, 136.3, 133.5, 127.2, 123.3, 122.0, 120.3, 120.0, 119.0,111.5, 111.0, 109.0, 103.5, 36.0, HR-EIMS *m/z*, calcd for $C_{17}H_{15}N_3O_3$ $[M]^+$ 309.1113 found 309.1102.

4.5. N′-(3,5-dihydroxybenzylidene)-2-(1H-indol-3-yl)acetohydrazide (3)

Yield: (84%); mp 284–286 °C; ^{1}HNMR (400 MHz, DMSO-d_6): δ 11.50 (s, 1H, NH), 11.12 (s, 1H, NH), 10.90 (s, 2H, OH), 7.92 (s, 1H), 7.72 (s, 1H), 7.35 (d, 2H, J = 8.0 Hz), 7.27 (t, 2H, J = 7.0 Hz), 6.92–6.86 (m, 3H), 3.69 (s, 2H, CH_2);^{13}CNMR (100, MHz, DMSO) δ171.0, 160.5, 160.5, 146.2, 136.3, 136.3, 127.2, 123.3, 122.0, 120.3, 119.0, 111.0, 109.0, 107.2, 107.2, 105.6, 36.0, HR-EIMS *m/z*, calcd for $C_{17}H_{15}N_3O_3$ $[M]^+$ 309.1113 found 309.1101.

4.6. 2-(1h-indol-3-yl)-N′-(2-methoxybenzylidene)acetohydrazide (4)

Yield: (87%); mp 229–231 °C match (Hanna et al., 2007; Ju et al., 2019; Liu et al., 2019; Mirfazli et al., 2016); ^{1}HNMR (400 MHz, DMSO-d_6): δ 11.64 (s, 1H, NH), 11.32 (s, 1H, NH), 8.35 (s, 1H), 7.94(s, 1H), 7.89 (d, 1H, J = 8.0 Hz), 7.71 (t, 1H, J = 7.0 Hz), 7.52 (t, 2H, J = 7.5 Hz), 6.85–6.80 (m, 4H), 3.92 (s, 3H, CH_3), 3.69 (s, 2H, CH_2);^{13}CNMR (100, MHz, DMSO) δ 171.0, 157.5, 146.2, 136.1, 132.1, 131.5, 127.2, 123.3, 122.0, 121.5, 120.3,119.0, 116.8, 111.2, 111.0, 109.0, 55.6, 36.0, HR-EIMS *m/z*, calcd for $C_{18}H_{17}N_3O_2$ $[M]^+$ 307.1321 found 307.1313.

4.7. N′-(3,4-dihydroxybenzylidene)-2-(1H-indol-3-yl)acetohydrazide(5)

Yield: (80%); mp 251–253 °C; ^{1}HNMR (400 MHz, DMSO-d_6): δ 11.29 (s, 1H, NH), 11.05 (s, 1H, NH), 10.92 (s, 1H, OH), 10.87 (s, 1H, OH), 7.95 (s, 1H), 7.74 (s, 1H), 7.53(d, 2H, J = 8.0 Hz), 7.36 (d, 2H, J = 8.0 Hz), 6.87–6.83 (m, 3H), 3.49 (s, 2H, CH_2);^{13}CNMR (100, MHz, DMSO) δ 171.0, 149.3, 146.8, 146.2, 136.1, 131.5, 127.2, 123.3, 123.0, 121.5, 120.3, 119.0, 117.5, 116.8, 111.0, 109.0, 36.0, HR-EIMS *m/z*, calcd for $C_{17}H_{15}N_3O_3$ $[M]^+$ 309.1113 found 309.1104.

4.8. N′-(2,5-dihydroxybenzylidene)-2-(1H-indol-3-yl)acetohydrazide (6)

Yield: (88%); mp 265–266 °C match (Hanna et al., 2007; Ju et al., 2019; Liu et al., 2019; Mirfazli et al., 2016); ^{1}HNMR (400 MHz, DMSO-d_6): δ 11.71 (s, 1H, NH), 11.18 (s, 1H, NH), 10.27 (s, 1H, OH), 9.92 (s, 1H, OH), 7.95 (s, 1H), 7.60 (t, 1H, J = 7.0 Hz), 7.34–30 (m, 2H), 7.12 (t, 2H, J = 8.0 Hz), 6.99–6.92 (m, 3H), 3.69 (s, 2H, CH_2);^{13}CNMR (100, MHz, DMSO) δ 171.0, 153.5, 151.3, 146.2, 136.1, 127.2, 123.3, 121.5, 120.3, 120.0, 119.8, 119.7, 119.0, 116.5, 111.0, 109.0, 36.0, HR-EIMS *m/z*, calcd for $C_{17}H_{15}N_3O_3$ $[M]^+$ 309.1113 found 309.1124.

4.9. N′-(3-hydroxybenzylidene)-2-(1H -indol-3-yl)acetohydrazide (7)

Yield: (82%); mp 261–263 °C match (Hanna et al., 2007; Ju et al., 2019; Liu et al., 2019; Mirfazli et al., 2016); ^{1}HNMR (400 MHz, DMSO-d_6): δ 11.46 (s, 1H, NH), 11.21 (s, 1H, NH), 9.42 (s, 1H, OH), 8.08 (s, 1H), 7.88 (s, 1H), 7.79 (d, 2H, J = 8.0 Hz), 7.32 (t, 1H, J = 7.0 Hz), 7.24–7.15 (m, 3H), 6.80–6.76 (m, 1H), 3.48 (s, 2H, CH_2);^{13}CNMR (100, MHz, DMSO) δ 171.0, 158.5, 146.2, 138.5,136.1, 130.3, 127.2, 123.3, 121.5, 121.3, 119.8, 118.5, 118.0, 114.8, 111.0, 109.0, 36.0, HR-EIMS *m/z*, calcd for $C_{17}H_{14}N_3O_2$ $[M]^+$ 293.1164 found 293.1152.

4.10. 2-(1 h-indol-3-yl)-N′-(2,4,6-trihydroxybenzylidene)acetohydrazide (8)

Yield: (80%); mp 294–296 °C; ^{1}HNMR (400 MHz, DMSO-d_6): δ 11.62 (s, 1H, NH), 10.92 (s, 2H, NH, OH), 10.26 (s, 2H, 2xOH), 8.32 (s, 1H), 7.64 (m, 2H), 7.42 (t, 2H, J = 7.0 Hz), 7.13 (d, 1H, J = 7.5 Hz), 6.62–6.86 (m, 2H), 3.69 (s, 2H, CH_2);^{13}CNMR (100, MHz, DMSO) δ 171.0, 164.0, 164.0, 163.7, 143.5, 136.1, 127.2, 123.3, 121.5, 119.5, 118.6, 111.0, 109.0, 106.4, 96.5, 96.5, 36.0, HR-EIMS *m/z*, calcd for $C_{17}H_{15}N_3O_4$ $[M]^+$ 325.1063 found 325.1051.

4.11. N′-(4-(dimethylamino)benzylidene)-2-(1H-indol-3-yl)acetohydrazide (9)

Yield: (80%); mp 295–296 °C; ^{1}HNMR (400 MHz, DMSO-d_6): δ 11.18 (s, 1H, NH), 10.93 (s, 1H, NH), 8.09 (s, 1H), 7.84(s, 1H), 7.54–7.47 (m, 2H), 7.41–7.32 (m, 2H), 7.29 (t, 2H, J = 7.0 Hz), 7.16 (d, 1H, J = 7.0 Hz), 3.54 (s, 2H, CH_2), 2.96 (s, 6H, $2XCH_3$),^{13}CNMR (100, MHz, DMSO) δ 171.0, 153.5, 144.3, 136.1, 128.5, 128.5, 127.2, 123.6, 123.3, 121.5, 120.0, 119.5, 118.6, 112.0, 111.0, 109.0, 41.5, 41.5, 36.0, HR-EIMS *m/z*, calcd for $C_{19}H_{20}N_4O$ $[M]^+$320.1637 found 320.1624.

4.12. 2-(1 h-indol-3-yl)-N′-(2-nitrobenzylidene)acetohydrazide(10)

Yield: (86%); mp 272–274 °C match (Hanna et al., 2007; Ju et al., 2019; Liu et al., 2019; Mirfazli et al., 2016); ^{1}HNMR (400 MHz, DMSO-d_6): δ 11.84 (s, 1H, NH), 11.54 (s, 1H, NH), 8.60 (s, 1H), 8.07–7.94 (m, 3H), 7.75–7.71(m, 2H), 7.54–7.50 (m, 2H), 7.02–6.96 (m, 2H), 3.56 (s, 2H, CH_2);^{13}CNMR (100, MHz, DMSO) δ 171.0, 148.0,143.5, 136.1, 134.7, 131.6, 130.4. 128.5, 127.2, 124.2,123.3, 121.5, 119.5, 118.6,111.0, 109.0, 36.0, HR-EIMS *m/z*, calcd for $C_{17}H_{14}N_4O_3$ $[M]^+$ 322.1066 found 322.1055.

4.13. 2-(1 h-indol-3-yl)-N′-(3-nitrobenzylidene)acetohydrazide(11)

Yield: (85%); mp 278–281 °C match (Hanna et al., 2007; Ju et al., 2019; Liu et al., 2019; Mirfazli et al., 2016); ^{1}HNMR (400 MHz, DMSO-d_6): δ 11.89 (s, 1H, NH), 11.64 (s, 1H, NH), 8.54 (s, 1H), 8.34 (s, 1H), 8.07–7.94 (m, 3H), 7.79 (t, 2H,

$J = 8.0$ Hz), 7.60 (t, 1H, $J = 7.0$ Hz), 6.92–6.86 (m, 2H), 3.58 (s, 2H, CH_2);^{13}CNMR (100, MHz, DMSO) δ 171.0, 148.2, 143.0, 136.1, 134.5, 132.8, 129.5, 127.2, 126.4, 123.3, 122.0, 121.6, 120.0, 119.5, 111.0, 109.0, 36.0, HR-EIMS *m/z*, calcd for $C_{17}H_{14}N_4O_3$ $[M]^+$ 322.1066 found 322.1053.

4.14. N′-(4-hydroxybenzylidene)-2-(1H-indol-3-yl)acetohydrazide(12)

Yield: (82%); mp 296–298 °C match (Hanna et al., 2007; Ju et al., 2019; Liu et al., 2019; Mirfazli et al., 2016); ^{1}HNMR (400 MHz, DMSO-d_6): δ 11.29 (s, 1H, NH), 11.05 (s, 1H, NH), 9.89 (s, 1H, OH), 8.08 (s, 1H),. 7.57–7.44 (m, 4H), 7.42 (t, 2H, $J = 7.0$ Hz), 7.26 (d, 2H, $J = 7.5$ Hz), 6.97–6.94 (m, 1H), 3.64 (s, 2H, CH_2);^{13}CNMR (100, MHz, DMSO) δ 171.0, 160.5, 144.3, 136.1, 130.4, 130.4, 127.2,126.5, 123.3, 121.6, 119.5, 118.6, 116.1, 116.1, 111.0, 109.0, 36.0, HR-EIMS *m/z*, calcd for $C_{17}H_{14}N_3O_2$ $[M]^+$ 293.1164 293.1164 found 293.1151.

4.15. N′-(4-chlorobenzylidene)-2-(1H-indol-3-yl)acetohydrazide(13)

Yield: (82%); mp 265–267 °C match (Hanna et al., 2007; Ju et al., 2019; Liu et al., 2019; Mirfazli et al., 2016); ^{1}HNMR (400 MHz, DMSO-d_6): δ 11.64 (s, 1H, NH), 11.44 (s, 1H, NH), 8.14 (s, 1H), 7.96 (s, 1H), 7.76–7.68 (m, 3H), 7.76–7.68 (m, 3H), 7.53–7.45 (m, 4H), 6.88 (t, 1H, $J = 7.0$ Hz), 3.67 (s, 2H, CH_2);^{13}CNMR (100, MHz, DMSO) δ 171.0, 144.3, 136.8, 136.4, 131.5, 130.5, 130.5, 128.4, 128.4, 127.2, 123.3, 121.6, 119.5, 118.6, 111.0, 109.0, 36.0, HR-EIMS *m/z*, calcd$C_{17}H_{14}ClN_3O$ for $[M]^+$ 311.0825 found 311.0811.

4.16. Methyl 4-((2-(2-(1H-indol-3-yl)acetyl)hydrazono)methyl)benzoate(14)

Yield: (87%); mp 302–304 °C; ^{1}HNMR (400 MHz, DMSO-d_6): δ 11.72 (s, 1H, NH), 11.43 (s, 1H, NH), 8.33 (s, 1H), 7.98–7.92 (m, 2H), 7.63 (d, 1H, $J = 7.0$ Hz), 7.22 (d, 2H, $J = 8.0$ Hz), 7.02 (t, 2H, $J = 7.0$ Hz), 3.82 (s, 3H, CH_3), 3.62 (s, 2H, CH_2);^{13}CNMR (100, MHz, DMSO) δ 171.0, 165.6, 144.3, 138.2, 136.8, 132.8, 130.3, 130.3, 129.4, 129.4, 127.2, 123.3, 121.6, 119.5, 118.6, 111.0, 109.0, 51.2, 36.0, HR-EIMS *m/z*, calcd for $C_{19}H_{17}N_3O_3$ $[M]^+$ 335.1270 found 335.1257.

4.17. 2-(1 h-indol-3-yl)-N′-(2-methylbenzylidene)acetohydrazide(15)

Yield: (83%); mp 224–226 °C; ^{1}HNMR (400 MHz, DMSO-d_6): δ 11.46 (s, 1H, NH), 11.16 (s, 1H, NH), 8.54 (s, 1H), 8.35 (s, 2H), 7.83–7.780 (m, 2H), 7.32–7.25 (m, 5H), 6.92–6.88 (m, 1H), 3.52 (s, 2H, CH_2), (s, 3H, CH_3); ^{13}CNMR (100, MHz, DMSO) δ 171.0, 143.0, 136.8, 135.5, 131.3, 130.5, 129.3, 127.2, 126.7, 125.9, 123.3, 121.6, 119.5, 118.6, 111.0, 109.0, 36.0, 19.0, HR-EIMS *m/z*, calcd for $C_{18}H_{17}N_3O$ $[M]^+$ 291.1372 found 291.1359.

4.18. 2-(1 h-indol-3-yl)-N′-(4-methylbenzylidene)acetohydrazide(16)

Yield: (84%); mp 232–233 °C; ^{1}HNMR (400 MHz, DMSO-d_6): δ 11.52 (s, 1H, NH), 11.18 (s, 1H, NH), 8.16 (s, 1H), 7.84 (d, 2H, $J = 8.0$ Hz), 7.69–7.62 (m, 4H), 7.06 (t, 1H, $J = 7.0$ Hz), 6.94 (d, 2H, $J = 8.0$ Hz), 3.68 (s, 2H, CH_2), 2.26 (m, 3H);^{13}CNMR (100, MHz, DMSO) δ 171.0, 144.3, 140.3, 136.8, 130.5, 129.4, 129.4, 127.2, 126.5, 126.5, 123.3, 121.6, 119.5, 118.6, 111.0, 109.0, 36.0. 21.5, HR-EIMS *m/z*, calcd for $C_{18}H_{17}N_3O$ $[M]^+$ 291.1372 found 291.1356.

4.19. N′-(3-chlorobenzylidene)-2-(1H-indol-3-yl)acetohydrazide(17)

Yield: (85%); mp 288–291 °C match (Hanna et al., 2007; Ju et al., 2019; Liu et al., 2019; Mirfazli et al., 2016); ^{1}HNMR (400 MHz, DMSO-d_6): δ 11.65 (s, 1H, NH), 11.45 (s, 1H, NH), 8.16 (s, 1H), 7.74 (d, 2H, $J = 8.0$ Hz),7.50–7.42 (m, 4H), 7.24–7.18 (m, 2H), 3.62 (s, 2H, CH_2);^{13}CNMR (100, MHz, DMSO) δ 171.0, 146.5, 136.8, 135.4, 134.6, 131.0, 130.5, 127.2, 127.2, 127.0, 123.3, 121.6, 119.5, 118.6, 111.0, 109.0, 36.0, HR-EIMS *m/z*, calcd for $C_{17}H_{14}$ Cl N_3O $[M]^+$ 311.0825 found 311.0814.

4.20. N′-(2-hydroxybenzylidene)-2-(1H-indol-3-yl)acetohydrazide(18)

Yield: (82%); mp 256–259 °C match (Hanna et al., 2007; Ju et al., 2019; Liu et al., 2019; Mirfazli et al., 2016); ^{1}HNMR (400 MHz, DMSO-d_6): δ 11.82 (s, 1H, NH), 11.23 (s, 1H, NH), 10.91 (s, 1H, OH), 8.14 (s, 1H), 7.57–7.49 (m, 2H), 7.46 (d, 1H, $J = 7.0$ Hz), 7.38–7.35 (m, 2H), 7.4–6.97 (m, 3H), 3.67 (s, 2H, CH_2);^{13}CNMR (100, MHz, DMSO) δ 171.0, 157.5, 146.3, 136.8, 132.0, 127.5, 127.2, 123.3, 121.6, 121.4, 119.5, 118.6, 118.4, 117.6, 111.0, 109.0, 36.0, HR-EIMS *m/z*, calcd for $C_{17}H_{14}N_3O_2$ $[M]^+$ 293.1164 found 293.1153.

4.21. 2-(1 h-indol-3-yl)-N′-(3-methylbenzylidene)acetohydrazide(19)

Yield: (83%); mp 226–228 °C; ^{1}HNMR (400 MHz, DMSO-d_6): δ11.51 (s, 1H, NH), 11.32 (s, 1H, NH), 8.14 (s, 1H), 7.53–7.49 (m, 3H), 7.38–7.35 (m, 4H), 6.84–6.86 (m, 2H), 3.57 (s, 2H, CH_2), 2.25 (s, 3H, CH_3); ^{13}CNMR (100, MHz, DMSO) δ 171.0, 146.5, 138.2, 136.8, 133.5, 131.8, 129.6, 128.4, 127.2, 126.6, 123.3, 121.6, 119.5, 118.6,111.0, 109.0, 36.0, 21.5, HR-EIMS *m/z*, calcd for $C_{18}H_{17}N_3O$ $[M]^+$ 291.1372 found 291.1359.

4.22. N′-(3-hydroxy-4-methoxybenzylidene)-2-(1H-indol-3-yl)acetohydrazide (20)

Yield: (81%); mp 248–250 °C match (Hanna et al., 2007; Ju et al., 2019; Liu et al., 2019; Mirfazli et al., 2016); ^{1}HNMR (400 MHz, DMSO-d_6): δ 11.06 (s, 1H, NH), 11.32 (s, 1H, NH), 9.48 (s, 1H, OH), 8.05 (s, 1H), 7.53 (d, 1H, $J = 7.0$ Hz), 7.32–7.28 (m, 4H), 7.03–6.92 (m, 3H), 3.82 (s, 3H, CH_3), 3.54 (s, 2H, CH_2);^{13}CNMR (100, MHz, DMSO) δ 171.0, 152.6, 147.6, 146.5,

136.8, 131.2, 127.2, 123.3, 122.0, 121.6, 119.5, 118.6, 115.7, 112.5, 111.0, 109.0, 56.3, 36.0. HR-EIMS *m/z*, calcd for $C_{18}H_{17}N_3O_3$ $[M]^+$ 323.1270 found 323.1257.

4.23. N′-(2,4-dimethoxybenzylidene)-2-(1H-indol-3-yl)acetohydrazide(21)

Yield: (83%); mp 304–306 °C; ^{1}HNMR (400 MHz, DMSO-d_6): δ 11.43 (s, 1H, NH), 11.12 (s, 1H, NH), 8.43 (s, 1H), 7.74 (d, 1H, $J = 7.5$ Hz), 7.65 (d, 1H, $J = 7.5$ Hz), 7.56–7.51 (m, 2H), 7.10 (d, 2H, $J = 7.5$ Hz), 6.59–6.53 (m, 2H), 3.81 (s, 6H, 2xCH_3), 3.56 (s, 2H, CH_2);^{13}CNMR (100, MHz, DMSO) δ 171.0, 163.4, 159.1, 146.5, 136.8, 133.2, 127.2, 123.3, 121.6, 119.5, 118.6, 111.0, 109.3, 109.0, 106.5, 101.8, 56.3, 56.3, 36.0, HR-EIMS *m/z*, calcd for $C_{19}H_{19}N_3O_3$ $[M]^+$ 337.1426 found 337.1413.

4.24. N′-(2,3-dihydroxybenzylidene)-2-(1H-indol-3-yl)acetohydrazide(22)

Yield: (85%); mp 229–231 °C match (Hanna et al., 2007; Ju et al., 2019; Liu et al., 2019; Mirfazli et al., 2016); ^{1}HNMR (400 MHz, DMSO-d_6): δ 11.74 (s, 2H, 2xNH), 11.26 (s, 1H, OH), 9.42 (s, 1H, OH) 8.24 (s, 1H), 7.62–7.58 (m, 2H), 7.52–7.47 (m, 4H), 7.13–7.08 (m, 2H), 3.55 (s, 2H, CH_2);^{13}CNMR (100, MHz, DMSO) δ 171.0, 151.5, 147.0, 146.5, 136.8, 127.2, 124.6, 123.3, 123.0, 121.6, 120.0, 120.0, 119.5, 118.6, 111.0, 109.0, 36.0, HR-EIMS *m/z*, calcd for $C_{17}H_{15}N_3O_3$ $[M]^+$ 309.1113 found 309.1103.

4.25. Molecular description

Molecular docking was performed as described by Khalid Zaman et al. (Krajewska, 2009) with slight modification. Docking had been performed by using AutoDock Vina (Mobley et al., 1995). A grid box size of 60 × 70 x 50 points had been set with a search spacing of 1 A°. Exhaustiveness parameter had been set to 500 while other parameters were left as default. The resulting best confirmation with most favourable free energy binding was selected for protein–ligand visualization. The 3D structure of compounds for docking had been prepared using Chem3D and optimized using MMFF94 forcefield (Li & Mobley, 2002). The results obtained from AutoDock Vina were analysed using Biovia Discovery Studio Visualizer.

5. Conclusion

In conclusion indole analogues (**1–22**) have been synthesized and characterized through ^{1}H-NMR, ^{13}C-NMR, HREI-MS successfully. All analogues were evaluated for urease inhibitory potential in search of lead candidates. All synthesized analogues showed a variable degree of inhibitory potential having IC_{50} value ranging between 0.60 ± 0.05 to 30.90 ± 0.90 μM when compared with standard drug thiourea having IC_{50} value 21.86 ± 0.90 μM. Compound **5** having 2-OH at C-3 and C-4 position was the most potent among the series showing strong binding interaction with active site of the enzyme, thus reducing the catalytic activity. The substitutions effects based on their number, position and nature on phenyl ring has been elaborated through structure activity relationship (SAR) study.

Acknowledgements

The authors acknowledged the financial supports By Deanship of scientific research through Project no. 2019-211-IRMC, Imam Abdulrahman Bin Faisal University (IAU), Saudi Arabia.

Disclosure statement

No potential conflict of interest was reported by the authors.

ORCID

Muhammad Taha http://orcid.org/0000-0003-3047-9289
Syahrul Imran http://orcid.org/0000-0001-7802-7359
Noor Barak Almandil http://orcid.org/0000-0002-7049-3563
Munther Alomari http://orcid.org/0000-0001-5705-2926
Fazal Rahim http://orcid.org/0000-0001-5856-4886
Bandar Alghanem http://orcid.org/0000-0002-3414-6580

References

Ali, B., Khan, K. M., Salar, U., Hussain, S., Ashraf, M., Riaz, M., Wadood, A., Taha, M., & Perveen, S. (2018). 1-[(4′-Chlorophenyl) carbonyl-4-(aryl) thiosemicarbazide derivatives as potent urease inhibitors: Synthesis, in vitro and in silico studies. *Bioorganic Chemistry*, *79*, 363–371. https://doi.org/10.1016/j.bioorg.2018.05.017

Ali, S., Ali, N., Dar, B. A., Pradhan, V., & Farooqui, M. (2013). Chemistry and biology of indoles and indazoles: A mini-review. *Mini Reviews in Medicinal Chemistry*, *13*(12), 1792–1800. https://doi.org/10.2174/1389557511313120009

Alomari, M., Taha, M., Imran, S., Jamil, W., Selvaraj, M., Uddin, N., & Rahim, F. (2019). Design, synthesis, in vitro evaluation, molecular docking and ADME properties studies of hybrid bis-coumarin with thiadiazole as a new inhibitor of Urease. *Bioorganic Chemistry*, *92*, 103235. https://doi.org/10.1016/j.bioorg.2019.103235

AmirJaved, M. S., & Kumar, H. (2008). Synthesis and biological evaluation of some 4-(1H-indol-3-yl)-6-phenyl-1,2,3,4-tetrahydropyrimidin-2-ones/thiones as potent anti-inflammatory agents. *Acta Pharmaceutica*, *58*(4), 467–477. https://doi.org/10.2478/v10007-008-0028-x

Aslam, M. A. S., Mahmood, S. U., Shahid, M., Saeed, A., & Iqbal, J. (2011). Synthesis, biological assay in vitro and molecular docking studies of new Schiff base derivatives as potential urease inhibitors. *European Journal of Medicinal Chemistry*, *46*(11), 5473–5479. https://doi.org/10.1016/j.ejmech.2011.09.009

Battaglia, S., Boldrini, E., Da Settimo, F., Dondio, G., La Motta, C., Marini, A. M., & Primofiore, G. (1999). Indole amide derivatives: Synthesis, structure–activity relationships and molecular modelling studies of a new series of histamine H1-receptor antagonists. *European Journal of Medicinal Chemistry*, *34*(2), 93–105. https://doi.org/10.1016/S0223-5234(99)80044-0

Bouchikhi, F., Rossignol, E., Sancelme, M., Aboab, B., Anizon, F., Fabbro, D., Prudhomme, M., & Moreau, P. (2008). Synthesis and biological evaluation of diversely substituted indolin-2-ones. *European Journal of Medicinal Chemistry*, *43*(11), 2316–2322. https://doi.org/10.1016/j.ejmech.2008.01.010

Chen, I., Safe, S., & Bjeldanes, L. (1996). Indole-3-carbinol and diindolylmethane as aryl hydrocarbon (Ah) receptor agonists and antagonists in T47D human breast cancer cells. *Biochemical Pharmacology*, *51*(8), 1069–1076. https://doi.org/10.1016/0006-2952(96)00060-3

Choppara, P., Bethu, M. S., Vara Prasad, Y., Venkateswara Rao, J., Uday Ranjan, T. J., Siva Prasad, G. V., Doradla, R., & Murthy, Y. L. N. (2019). Synthesis, characterization and cytotoxic investigations of

novel bis (indole) analogues besides antimicrobial study. *Arabian Journal of Chemistry*, *12*(8), 2721–2731. https://doi.org/10.1016/j.arabjc.2015.05.015

de Fátima, Â., de Paula Pereira, C., Olímpio, C. R., de Freitas Oliveira, B. G., Franco, L. L., & da Silva, P. H. C. (2018). Schiff bases and their metal complexes as urease inhibitors – A brief review. *Journal of Advanced Research*, *13*, 113–126. https://doi.org/10.1016/j.jare.2018.03.007

de Oliveira Moraes, A. D. T., de Miranda, M. D. S., Jacob, Í. T. T., da Cruz Amorim, C. A., de Moura, R. O., da Silva, S. Â. S., Soares, M. B. P., de Almeida, S. M. V., de Lima Souza, T. R. C., de Oliveira, J. F., da Silva, T. G., de Melo, C. M. L., Moreira, D. R. M., & de Lima, M. d. C. A. (2018). Synthesis, in vitro and in vivo biological evaluation, COX-1/2 inhibition and molecular docking study of indole-N-acylhydrazone derivatives. *Bioorganic & Medicinal Chemistry* 26: 5388–5396.

Dharmendra, K., Narendra, K., Tarun, S., & Singh, C. P. (2010). Synthesis of pharmacologically active 2- phenyl sulpha/substituted indoles. *International Journal of Engineering, Science and Technology*, *2*(7), 2553–2557.

Douglass, F., Taber, K., & Pavan, T. J. (2011). Indole synthesis: A review and proposed classification. *Tetrahedron*, *67*(38), 7195–7210. https://doi.org/10.1016/j.tet.2011.06.040

Gribble, G. W. (2000). Recent developments in indole ring synthesis-methodology and applications. *Journal of the Chemical Society, Perkin Transactions 1*, *1*(7), 1045–1075. https://doi.org/10.1039/a909834h

Guerra, A. S. H. d. S., Malta, D. J. d. N., Laranjeira, L. P. M., Maia, M. B. S., Colaço, N. C., de Lima, M. d. C. A., Galdino, S. L., Pitta, I. d. R., & Gonçalves-Silva, T. (2011). Anti-inflammatory and antinociceptive activities of indole-imidazolidine derivatives. *International Immunopharmacology*, *11*(11), 1816–1822. https://doi.org/10.1016/j.intimp.2011.07.010

Hanna, M. L., Tarasow, T. M., & Perkins, J. (2007). Mechanistic differences between in vitro assays for hydrazone-based small molecule inhibitors of anthrax lethal factor. *Bioorganic Chemistry*, *35*(1), 50–58. https://doi.org/10.1016/j.bioorg.2006.07.004

Hiari, Y. M., Qaisi, A. M., Abadelah, M., & Voelter, M. W. (2006). Synthesis and antibacterial activity of some substituted 3-(Aryl)- and 3-(hetero-aryl)indoles. *Monatshefte für Chemie - Chemical Monthly*, *137*(2), 243–248. https://doi.org/10.1007/s00706-005-0424-6

Ju, Z., Su, M., Hong, J., La Kim, E., Moon, H. R., Chung, H. Y., Kim, S., & Jung, J. H. (2019). Design of balanced COX inhibitors based on anti-inflammatory and/or COX-2 inhibitory ascidian metabolites. *European Journal of Medicinal Chemistry*, *180*, 86–98. https://doi.org/10.1016/j.ejmech.2019.07.016

Karadeniz, A., Kaya, B., Savaş, B., & Topcuoğlu, Ş. F. (2011). Effects of two plant growth regulators, indole-3-acetic acid and β-naphthoxyacetic acid, on genotoxicity in Drosophila SMART assay and on proliferation and viability of HEK293 cells from the perspective of carcinogenesis. *Toxicology and Industrial Health*, *27*(9), 840–848. https://doi.org/10.1177/0748233711399314

Kassab, A. E., & Hassan, R. A. (2018). Novel benzotriazole N-acylarylhydrazone hybrids: Design, synthesis, anticancer activity, effects on cell cycle profile, caspase-3 mediated apoptosis and FAK inhibition. *Bioorganic Chemistry*, *80*, 531–544. https://doi.org/10.1016/j.bioorg.2018.07.008

Khan, K., Naz, M. F., Taha, M., Khan, Perveen, A. S., Choudhary, M., & Voelter, I. W. (2014). Synthesis and in vitro urease inhibitory activity of N,N′-disubstituted thioureas. *European Journal of Medicinal Chemistry*, *74*, 314–323. https://doi.org/10.1016/j.ejmech.2014.01.001

Krajewska, B. (2009). Ureases I. Functional, catalytic and kinetic properties: A review. *Journal of Molecular Catalysis B: Enzymatic*, *59*(1-3), 9–21. https://doi.org/10.1016/j.molcatb.2009.01.003

Kwon-Chung, K. J., Fraser, J. A., Doering, T. L., Wang, Z. A., Janbon, G., Idnurm, A., & Bahn, Y. S. (2014). Cryptococcus neoformans and *Cryptococcus gattii*, the etiologic agents of cryptococcosis. *Cold Spring Harbor Perspectives in Medicine*, *4*(7), a019760. https://doi.org/10.1101/cshperspect.a019760

Li, X., & Mobley, H. L. (2002). Vaccines for Proteus mirabilis in urinary tract infection. *International Journal of Antimicrobial Agents*, *19*(6), 461–465. https://doi.org/10.1016/S0924-8579(02)00102-4

Liu, B., Li, R., Li, Y., Li, S., Yu, J., Zhao, B., Liao, A., Wang, Y., Wang, Z., Lu, A., Liu, Y., & Wang, Q. (2019). Discovery of pimprinine alkaloids as novel agents against a plant virus. *Journal of Agricultural and Food Chemistry*, *67*(7), 1795–1806. https://doi.org/10.1021/acs.jafc.8b06175

Lucas, J., Menschen, A., Lottspeich, F., Voegeli, U., & Boiler, T. (1985). Amino-terminal sequence of ethylene-induced bean leaf chitinase reveals similarities to sugar-binding domains of wheat germ agglutinin. *FEBS Letters*, *193*(2), 208–210. https://doi.org/10.1016/0014-5793(85)80152-6

Mirfazli, S. S., Khoshneviszadeh, M., Jeiroudi, M., Foroumadi, A., Kobarfard, F., & Shafiee, A. (2016). Design, synthesis and QSAR study of arylidene indoles as anti-platelet aggregation inhibitors. *Medicinal Chemistry Research*, *25*(1), 1–18. https://doi.org/10.1007/s00044-015-1440-7

Mobley, H. (1996). The role of Helicobacter pylori urease in the pathogenesis of gastritis and peptic ulceration. *Alimentary Pharmacology & Therapeutics*, *10*(Sup1), 57–64. https://doi.org/10.1046/j.1365-2036.1996.22164006.x

Mobley, H., Island, M. D., & Hausinger, R. P. (1995). Molecular biology of microbial ureases. *Microbiological Reviews*, *59*(3), 451–480. https://doi.org/10.1128/MMBR.59.3.451-480.1995

Naureen, S., Chaudhry, F., Asif, N., Munawar, M. A., Ashraf, M., Nasim, F. H., Arshad, H., & Khan, M. A. (2015). Discovery of indole-based tetraarylimidazoles as potent inhibitors of urease with low antilipoxygenase activity. *European Journal of Medicinal Chemistry*, *102*, 464–470. https://doi.org/10.1016/j.ejmech.2015.08.011

Odake, S., Morikawa, T., Tsuchiya, M., Imamura, L., & Kobashi, K. (1994). Inhibition of *Helicobacter pylori* urease activity by hydroxamic acid derivatives. *Biological & Pharmaceutical Bulletin*, *17*(10), 1329–1332. https://doi.org/10.1248/bpb.17.1329

Olivera-Severo, D., Wassermann, G. E., & Carlini, C. R. (2006). Ureases display biological effects independent of enzymatic activity: Is there a connection to diseases caused by urease-producing bacteria?. *Brazilian Journal of Medical and Biological Research = Revista Brasileira de Pesquisas Medicas e Biologicas*, *39*(7), 851–861. https://doi.org/10.1590/s0100-879x2006000700002

Omar, F. A., Mahfouz, N. M., & Rahman, M. A. (1996). Design, synthesis and anti-inflammatory activity of some 1,3,4-oxadiazole derivatives. *European Journal of Medicinal Chemistry*, *31*(10), 819–825. https://doi.org/10.1016/0223-5234(96)83976-6

Pandeya, N., Yogeeswari, P., Ram, D., & Nath, S. G. (1998). Synthesis and antimicrobial activity of N-Mannich bases of 3-[N′-sulphadoximino] isatin and its methyl derivative. *Bollettino Chimico Farmaceutico*, *137*(8), 321–324.

Parklmamura, J. L., & Kobashi, K. (1996). Kinetic studies of *Helicobacter pylori* urease inhibition by a novel proton pump inhibitor, rabeprazole. *Biological & Pharmaceutical Bulletin*, *19*(2), 182–187. https://doi.org/10.1248/bpb.19.182

Poeggeler, B., Reiter, R. J., Tan, D. X., Chen, L. D., & Manchester, L. C. (1993). Melatonin, hydroxyl radical-mediated oxidative damage, and aging: A hypothesis . *Journal of Pineal Research*, *14*(4), 151–168. https://doi.org/10.1111/j.1600-079x.1993.tb00498.x

Przheval'skii, N. M., Magedov, I. V., & Drozd, V. N. (1997). New derivatives of indole. Synthesis of s-(indolyl-3) diethyl dithiocarbamates. *Chemistry of Heterocyclic Compounds*, *33*(12), 1475–1476. https://doi.org/10.1007/BF02291655

Saify, Z. S., Kamil, A., Akhtar, S., Taha, M., Khan, A., Khan, K. M., Jahan, S., Rahim, F., Perveen, S., & Choudhary, M. I. (2014). 2-(2′-Pyridyl) benzimidazole derivatives and their urease inhibitory activity. *Medicinal Chemistry Research*, *23*(10), 4447–4454. https://doi.org/10.1007/s00044-014-1015-z

Schmidt, S., Preu, L., Lemcke, T., Totzke, F., Schächtele, C., Kubbutat, M. H., & Kunick, C. (2011). Dual IGF-1R/SRC inhibitors based on a N′-aroyl-2-(1H-indol-3-yl)-2-oxoacetohydrazide structure. *European Journal of Medicinal Chemistry*, *46*(7), 2759–2769. https://doi.org/10.1016/j.ejmech.2011.03.065

Seraj, F., Kanwal, Khan, K. M., Khan, A., Ali, M., Khalil, R., Ul-Haq, Z., Hameed, S., Taha, M., Salar, U., & Perveen, S. (2021). Biology-oriented drug synthesis (BIODS), in vitro urease inhibitory activity, and in silico

studies on ibuprofen derivatives. *Molecular Diversity*, *25*(1), 143–157. https://doi.org/10.1007/s11030-019-10032-x 31965436

Sharma, V., Bhatia, P., Alam, O., Naim, M. J., Nawaz, F., Sheikh, A. A., & Jha, M. (2019). Recent advancement in the discovery and development of cox-2 inhibitors: Insight into biological activities and sar studies (2008-2019)). *Bioorganic Chemistry*, *89*(2019), 103007. https://doi.org/10.1016/j.bioorg.2019.103007

Siddiqui, N., Alam, M., & Ahsan, W. (2008). Synthesis, anticonvulsant and toxicity evaluation of 2-(1*H*-indol-3-yl)acetyl-N-(substituted phenyl)hydrazine carbothioamides and their related heterocyclic derivatives. *Acta Pharmaceutica*, *58*(4), 445–454. https://doi.org/10.2478/v10007-008-0025-0

SuzenBuyukbingol, S. E. (1998). Evaluation of anti-HIV activity of 5-(2-phenyl-3′-indolal)-2-thiohydantoin. *Il Farmaco*, *53*(7), 525–527. https://doi.org/10.1016/S0014-827X(98)00053-6

Taha, M., & Wadood, A. (2018). Synthesis and molecular docking study of piperazine derivatives as potent urease inhibitors. *Bioorganic Chemistry*, *78*, 411–417. https://doi.org/10.1016/j.bioorg.2018.04.007

Taha, M., Aldhamin, E. A. J., Almandil, N. B., Anouar, E. H., Uddin, N., Alomari, M., Rahim, F., Adalat, B., Ibrahim, M., Nawaz, F., Iqbal, N., Alghanem, B., Altolayyan, A., & Khan, K. M. (2020). Synthesis of indole based acetohydrazide analogs: Their in vitro and in silico thymidine phosphorylase studies. *Bioorganic Chemistry*, *98*, 103745. https://doi.org/10.1016/j.bioorg.2020.103745

Taha, M., Ismail, N. H., Baharudin, M. S., Lalani, S., Mehboob, S., Khan, K. M., Yousuf, S., Siddiqui, S., Rahim, F., & Choudhary, M. I. (2015). Synthesis crystal structure of 2-methoxybenzoylhydrazones and evaluation of their α-glucosidase and urease inhibition potential. *Medicinal Chemistry Research*, *24*(3), 1310–1324. https://doi.org/10.1007/s00044-014-1213-8

Taha, M., Ismail, N. H., Imran, S., Wadood, A., Rahim, F., & Riaz, M. (2015). Synthesis of potent urease inhibitors based on disulfide scaffold and their molecular docking studies. *Bioorganic & Medicinal Chemistry*, *23*(22), 7211–7218. https://doi.org/10.1016/j.bmc.2015.10.017

Taha, M., Shah, S. A. A., Khan, A., Arshad, F., Ismail, N. H., Afifi, M., Imran, S., & Choudhary, M. I. (2019). Synthesis of 3, 4, 5-trihydroxybenzohydrazone and evaluation of their urease inhibition potential. *Arabian Journal of Chemistry.*, *12*(8), 2973–2982. https://doi.org/10.1016/j.arabjc.2015.06.036

Tantak, M. P., Klingler, L., Arun, V., Kumar, A., Sadana, R., & Kumar, D. (2017). Design and synthesis of bis(indolyl)ketohydrazide-hydrazones: Identification of potent and selective novel tubulin inhibitors. *European Journal of Medicinal Chemistry*, *136*, 184–194. https://doi.org/10.1016/j.ejmech.2017.04.078

Van Order, R. B., & Lindwall, H. G. (1942). Indole. *Chemical Reviews*, *30*(1), 69–96. https://doi.org/10.1021/cr60095a004

Wahid, S., Jahangir, S., Versiani, M. A., Khan, K. M., Salar, U., Ashraf, Farzand, M. U., Wadood, A., Taha, M., & Perveen, S. (2020). Atenolol thiourea hybrid as potent urease inhibitors: Design, biology-oriented drug synthesis, inhibitory activity screening, and molecular docking studies. *Bioorganic Chemistry*, *94*, 103359. https://doi.org/10.1016/j.bioorg.2019.103359

Wani, T. A., Bakheit, A. H., Zargar, S., Bhat, M. A., & Al-Majed, A. A. (2019). Molecular docking and experimental investigation of new indole derivative cyclooxygenase inhibitor to probe its binding mechanism with bovine serum albumin. *Bioorganic Chemistry*, *89*, 103010. https://doi.org/10.1016/j.bioorg.2019.103010

Zaman, K., Rahim, F., Taha, M., Ullah, H., Wadood, A., Nawaz, M., Khan, F., Wahab, Z., Shah, S. A., Rehman, A. U., Kawde, A. N., & Gollapalli, M. (2019). Synthesis, in vitro urease inhibitory potential and molecular docking study of benzimidazole analogues. *Bioorganic Chemistry*, *89*, 103024. https://doi.org/10.1016/j.bioorg.2019.103024